Colloquium: Water's controversial glass transitions

Katrin Amann-Winkel[*]
Institute of Physical Chemistry, University of Innsbruck, 6020 Innsbruck, Austria

Roland Böhmer
Fakultät Physik, Technische Universität Dortmund, 44221 Dortmund, Germany

Franz Fujara
Institut für Festkörperphysik, Technische Universität Darmstadt, 64289 Darmstadt, Germany

Catalin Gainaru[†]
Fakultät Physik, Technische Universität Dortmund, 44221 Dortmund, Germany

Burkhard Geil
Institut für Physikalische Chemie, Georg August-Universität Göttingen, 37077 Göttingen, Germany

Thomas Loerting
Institute of Physical Chemistry, University of Innsbruck, 6020 Innsbruck, Austria

(published 17 February 2016)

Water is the most common and, judged from its numerous anomalous properties, the weirdest of all known liquids and the complexity of its pressure-temperature map is unsurpassed. A major obstacle on the way to a full understanding of water's structure and dynamics is the hard-to-explore territory within this map, colloquially named the no man's land. Many experiments suggest that just before stepping across its low-temperature border, amorphous ices undergo glass-to-liquid transitions while other interpretations emphasize the importance of underlying disordered (nano)crystalline states. Prospects for reconciling the conflicting views regarding the nature of water's glass transitions are discussed.

DOI: 10.1103/RevModPhys.88.011002

CONTENTS

I. INTRODUCTION

Water's density maximum at 4 °C is recognized at least since the days of Galileo (Brovchenko and Oleinikova, 2008) and we all know how this anomaly helps to preserve aquatic life during harsh winters. While this unusual temperature dependence of density distinguishes water from virtually all other liquids, it is just one among a zoo of currently more than 70 anomalous manifestations[1] so far reported to occur for this most ubiquitous and strangest of all fluids. These anomalies shape the face of Earth and are at the core of water's role as a

[*]Present address: Department of Physics, AlbaNova University Center, Stockholm University, 10691 Stockholm, Sweden.

[†]Present address: Department of Chemistry, University of Tennessee, Knoxville, TN 37996, USA.

[1]Chaplin, M., Water Structure and Science, http://www.lsbu.ac.uk/water/.

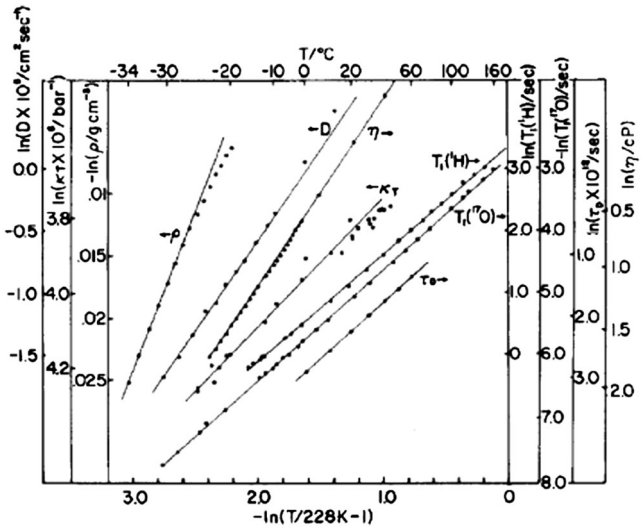

FIG. 1. Several water properties represented in a double-logarithmic plot suggesting power-law behavior of (from left to right) density ρ, diffusion coefficient D, shear viscosity η, isothermal compressibility κ_T, proton and oxygen spin-lattice relaxation time T_1, and dielectric relaxation time τ_D. This set of data is drawn to imply an extrapolated divergence of all quantities near 228 K. Note that even the density measurements approach this temperature only within 10 K. From Speedy and Angell, 1976.

"matrix of life,"[2] while their microscopic origin remains elusive and poorly understood even today, despite intensive research effort.

The key to resolving this long-standing puzzle is Fahrenheit's (1724) time honored observation that water can stay liquid upon cooling to temperatures below 0 °C, and then with increasing degree of supercooling continues to expand at ever growing rates. As illustrated in Fig. 1 the thermal expansivity and many other quantities tend to diverge at about −45 °C (228 K) at ambient pressure. However, the existence of this metastable state of water is terminated *prior* to reaching the incipient divergence within a margin of just a few Kelvin (Speedy and Angell, 1976).

Ice is spontaneously (or homogeneously) nucleated within supercooled water near a temperature T_H of about 235 K. The ensuing rapid crystallization has hampered many laboratory studies so that it remains unclear whether the extrapolated divergence is real, so far precluding direct exploration of the state of matter that would emerge much below T_H. Application of pressures up to 2 kbar (0.2 GPa) can reduce T_H by another ≈50 K. Yet, also under conditions of high compression an apparently inevitable crystallization impedes efforts to step across what Mishima and Stanley (1998b) called water's "no man's land." The persisting experimental challenge is to try and circumvent this frontier, for instance by using smaller sample volumes and/or by probing shorter time scales while still sensing the behavior of bulk water. Computer simulations provide a suitable means to overcome these constraints if appropriate water models are examined: A prominent example was given by Poole *et al.* (1992) who suggested the existence of a liquid-liquid critical point in addition to water's well-known liquid-vapor critical point, a scenario provoking heated debates since it was conceived.

With the idea to preserve the disordered structure of the high-temperature ($T > T_H$) liquid, one may aim at arresting large-scale motions of the H_2O molecules and thus produce a noncrystalline, i.e., glassy water solid. Nature implemented a related idea long before we did: In the Universe water exists predominantly as noncrystalline frost, condensed as vapor on interstellar dust grains (Jenniskens and Blake, 1996).

A large number of routes were devised to produce glassy water in the laboratory: Apart from depositing water vapor on cold substrates, vitrification of micron-sized water droplets by hyperquenching is often exploited. Amorphization of crystalline ice by means of, e.g., high pressure or radiation damage represents yet another strategy. The diverse preparation techniques yield noncrystalline ices with ambient-pressure densities that can greatly vary from 0.3 to 1.3 g/cm^3 (Loerting *et al.*, 2011). At ambient pressure and for heating rates of 1 K/s or less all of the amorphous ices crystallize at temperatures T_X near 150 K. Those with low densities ($\rho < 0.95$ g/cm) crystallize directly into what is called cubic ice, but more compact, high-density amorphous (HDA) ices with $\rho > 1.12$ g/cm^3 first transform into a low-density amorph (LDA) at temperatures between 105 and 135 K, depending on sample history. Although debated for a long time, agreement appears to emerge that LDA undergoes a transition into a thawed state at a calorimetric glass transition temperature T_g near 136 K before transforming to cubic ice.

Whether or not LDA's glass transition is to be thought of in direct analogy to the phenomenon occurring upon window glass softening remains unclear. In Sec. V, we review apparently conflicting experimental evidence which resulted in a divided opinion on this issue. Provided the glass transition leads to ultraviscous liquid water and the constituent molecules thus perform rotational *and* translational motions, then does this state of matter correspond to the metastable liquid that we have lost track of just above T_H? If so, it is conceivable that there might be a continuous thermodynamic bridge (Johari *et al.*, 1994) leading across the no man's land, and it is worthwhile to explore whether the high- and low-density amorphous polymorphs are related to the two liquid forms of water (Poole *et al.*, 1992) alluded to previously.

Alternatively, one may argue that the oxygen atoms in the amorphous ices set up a network which remains essentially unaffected by the glass transition so that above T_g only proton motion prevails. This latter scenario is more akin to the situation encountered in magnetic spin glasses (Binder and Young, 1986) and their nonmagnetic analogs, the orientational glasses (Höchli, Knorr, and Loidl, 1990).

Based on the selection of experimental data that we are able to discuss within the format of this Colloquium, its main purpose is a critical assessment of the different scenarios. It turns out that some of the controversies might be brought to resolution by paying more explicit attention to the nature of the amorphous ice samples used in the experimental studies. To illustrate the idea of the underlying discussion in a

[2]Ball, P., 1999, H_2O: Biography of water (Weidenfeld and Nicolson), provides an amusing and informative reading on water. Finney, J. L., 2015, Water—A very short introduction (Oxford University Press) provides an excellent introduction to the topic.

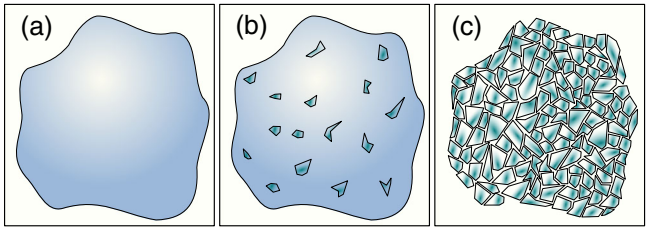

FIG. 2. Sketches of three different ideas put forward to understand amorphous ices either (a) as purely glassy materials, (b) as nanocrystalline domains embedded in a glassy matrix, or (c) as purely nanocrystalline.

simplified manner Fig. 2 distinguishes three scenarios of potential use for an understanding of x-ray amorphous ice samples. These may either be completely glassy, entirely nanocrystalline, or be best represented as nanocrystallites embedded in a glassy matrix. We anticipate here, though, that the scenario sketched in Fig. 2(c)—long discussed for inorganic glasses as well (Phillips, 1982) and eventually put aside—could not be substantiated for any of the amorphous ices studied so far.

II. PHASE DIAGRAM OF NONCRYSTALLINE WATER

What is at the core of the incipient divergence inferable from the work of Speedy and Angell (1976); cf. Fig. 1? Forty years of intensive and clever experimental and theoretical research effort were not enough to yield generally accepted answers regarding this issue. Although this Colloquium focuses on the range below the low-temperature end of the no man's land, a look at and beyond its high-temperature frontier is warranted in the quest of understanding whether and then how the supercooled and the glassy regions in water's phase diagram might be connected. In view of excellent reviews that treat these matters comprehensively (Angell, 1982; Mishima and Stanley, 1998b; Debenedetti, 2003; Soper, 2008; Caupin, 2015), here we deal with only a few recent aspects. The major difficulty in exploring no man's land is the enhanced crystallization tendency which, however, can be (partially) circumvented by working on very short time scales or by using very small sample volumes.

To bring us to the edge of the problem it is instructive to examine the schematic pressure-temperature phase diagram of noncrystalline water that is presented in Fig. 3. Let us start from those regimes of this diagram known from textbooks and then go on to explore its metastable regimes. In Fig. 3 the boiling line T_B and the melting line T_M reflect well-known two-phase coexistence lines, each corresponding to equal Gibbs free energies of the associated water phases. Together with the sublimation line the three binodals meet in the triple point. The melting and the sublimation lines are missing in Fig. 3 because crystalline ice is excluded from the phase diagram of noncrystalline water. The liquid-vapor line T_B at which, e.g., the specific heat and the isothermal compressibility diverge, terminates in the critical point C_1. Beyond C_1, in the supercritical fluid in which liquid and gaseous water are indistinguishable, "shadows" of the liquid-vapor line continue in the form of Widom lines. When stepping across

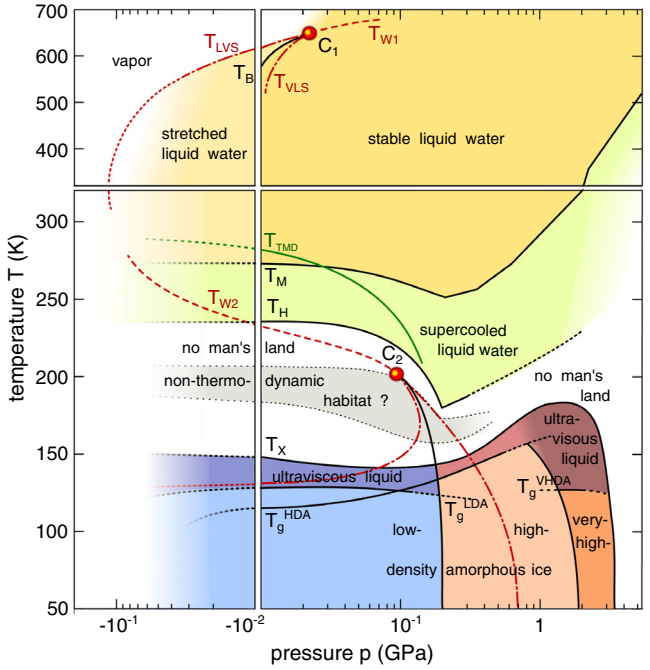

FIG. 3. Schematic pressure-temperature phase diagram of noncrystalline water. To be able to show large ranges of stretched ($p < 0$) and compressed ($p > 0$) water we choose a logarithmic pressure axis that hides the $|p| \approx 0$ range. Likewise, the high-temperature regime is shown on a compressed scale. Near its upper end, the boiling line T_B terminates in the critical point C_1. The long-dashed lines T_{W1} and T_{W2} mark Widom lines and the dash-dotted lines represent spinodals. The Widom line T_{W2}, emanating from the debated liquid-liquid critical point C_2 may alternatively be read as Speedy's (1982) retracing spinodal. Other acronyms include T_{LVS} for liquid-vapor spinodal, T_{VLS} for vapor-liquid spinodal, T_M for melting temperature, T_{TMD} for temperature of maximum density, T_H for homogeneous nucleation temperature, T_X for crystallization temperature, and T_g for the glass transition temperatures of various amorphous ices. The LDA-HDA boundary reflects an average of upstroke and downstroke transitions both of which are sharp and first-order-like. Because of this hysteresis LDA can be studied in (parts of) the HDA domain and vice versa. The HDA-VHDA (very high-density amorphous ice) boundary reflects the (continuous or weakly discontinuous) upstroke transition. Dotted lines represent suggestions or results of extrapolations. Several of the "phase" boundaries follow those summarized, e.g., by Stanley *et al.* (2000), Klotz *et al.* (2003), Klotz, Strässle, Saitta *et al.* (2005), Soper (2008), and Caupin (2015). The word *phase* is used here for convenience and should not be taken to imply that each state referred to in this diagram corresponds to a phase in the thermodynamic sense.

them, maxima rather than singularities occur in various dynamic and thermodynamic quantities enabling one to track these lines (Simeoni *et al.*, 2010), here for simplicity represented by a single line T_{W1}. For pressures and temperatures just below the critical point, the liquid state becomes first *metastable* against vaporization when traversing the liquid-vapor binodal T_B and then also *unstable* upon crossing the liquid-vapor spinodal T_{LVS}. Below about 600 K T_{LVS} extends well into the negative-pressure domain. Upon inspecting

water's equation of state Speedy (1982) suggested that the extrapolated spinodal attains a minimum pressure when approaching the extrapolated liquid-density maximum line T_{TMD}; cf. Fig. 3. In addition, Speedy conjectured that toward lower temperatures the spinodal traces back to positive pressures and that this would rationalize the stability limit suggested by the data in Fig. 1. On thermodynamic grounds Debenedetti (2003) argued that even if the liquid-vapor spinodal displayed nonmonotonic behavior, it should not retrace all the way to positive pressures thus essentially ruling out Speedy's stability limit conjecture.

Another intriguing possibility to explain water's anomalous properties was raised almost 25 years ago when Poole *et al.* (1992) interpreted their computer simulations of a water model in terms of the existence of a liquid-liquid critical point (LLCP) just within the no man's land; see Fig. 3 for its potential location. According to their findings, a tetrahedrally coordinated low-density liquid should coexist with a less structured liquid of higher density at temperatures below the LLCP so that above it the fraction of temporarily existing low-density water patches decreases and the liquid contracts upon heating. This view pictures supercooled and stable water as a supercritical mixture of high- and low-density components.

As already pointed out by Poole *et al.* (1992) the consequences of an experimentally inaccessible LLCP could nevertheless be monitored from a distance: For temperatures below the no man's land the extrapolated coexistence curve would rationalize the occurrence of high-density and low-density amorphous states as the vitrified counterparts of each of the two fluids suggested by Mishima and Stanley (1998a, 1998b) to exist near the LLCP. Provided the LLCP is positioned as implied by Fig. 3, then the Widom line emanating from it could become observable if it quits the no man's land in the negative-pressure domain (Caupin, 2015).

Many variants of water's phase diagram were proposed by Pallares *et al.* (2014), regarding the upper left portion of the diagram shown in Fig. 3. To rationalize recent cavitation experiments on metastable water, Tanaka (1996) and Angell (2014) considered "pulling down" the LLCP into the negative-pressure regime (e.g., along the T_{W2} line). Singularity-free scenarios were devised (Sastry *et al.*, 1996) and refined (Debenedetti, 2003; Angell, 2008) that avoid the existence of an LLCP while retaining reference to two distinguishable metastable liquids. Whether really two liquid phases have been identified in computer experiments (Paschek, Rüppert, and Geiger, 2008; Poole *et al.*, 2013; Holten *et al.*, 2014; Palmer, Martelli *et al.*, 2014; Palmer, Debenedetti *et al.*, 2014) or not (Limmer and Chandler, 2011, 2013) is currently vigorously debated. In particular, Chandler (2014) questioned that the low-density liquid represents a sufficiently equilibrated phase and argued that it merely reflects transient local fluctuations bound to crystallize prematurely, i.e., before water's structural relaxation is complete. Conversely, Monte Carlo simulations by Brovchenko, Geiger, and Oleinikova (2003, 2005) reported on evidence for three or more supercooled liquids.

Before revisiting this issue in Sec. III, we now inspect the complexities that await us at temperatures below the no man's land's lower border. When focusing on the range below, e.g., 100 K, for increasing (positive) pressures, according to Fig. 3 we encounter a sequence of three amorphous states: LDA, HDA, and very-high-density amorphous ice (VHDA, with $\rho \approx 1.26\ \mathrm{g/cm^3}$). This phenomenon, so far discovered for only a handful of substances (McMillan *et al.*, 2007), is known as "amorphous polymorphism" or "polyamorphism." It rationalizes the course of the amorphous ices' nonmonotonic crystallization line T_X (see Fig. 3), which passes through a minimum near 0.2 GPa, a pressure at which HDA becomes more stable than LDA, and then this line exhibits a maximum near 2 GPa where VHDA is most stable. At still larger pressures T_X drops precipitously so that VHDA, when compressed to $p > 3.5$ GPa at 77 K, yields ice VIII (Klotz *et al.*, 2003). Prior to reaching the crystallization boundary, LDA, HDA, and VHDA (treated as outlined in Sec. IV) all display glass transitions at temperatures $T_g(p)$. T_g^{LDA} decreases (Giovambattista *et al.*, 2012) and T_g^{HDA} increases (Loerting *et al.*, 2015) with pressure, while T_g^{VHDA} is largely pressure insensitive and relatively low (Handle and Loerting, 2016). The HDA↔LDA boundary, which Whalley *et al.* (1987) located near 0.2 GPa, owing to its large hysteresis (Mishima, 1994) deserves special attention. In Fig. 3 the HDA → LDA and LDA → HDA stability limits are tentatively identified with spinodals emanating from the debated LLCP.

When inspecting the crystallization products in Fig. 4, a link between the amorphous ices and liquid water is suggested: Both of them cease to exist above ∼4 GPa. As indicated by the arrows in Fig. 4 the isobaric crystallization products of supercooled liquid water near T_H and amorphous ices near T_X (where they may or may not be ultraviscous,

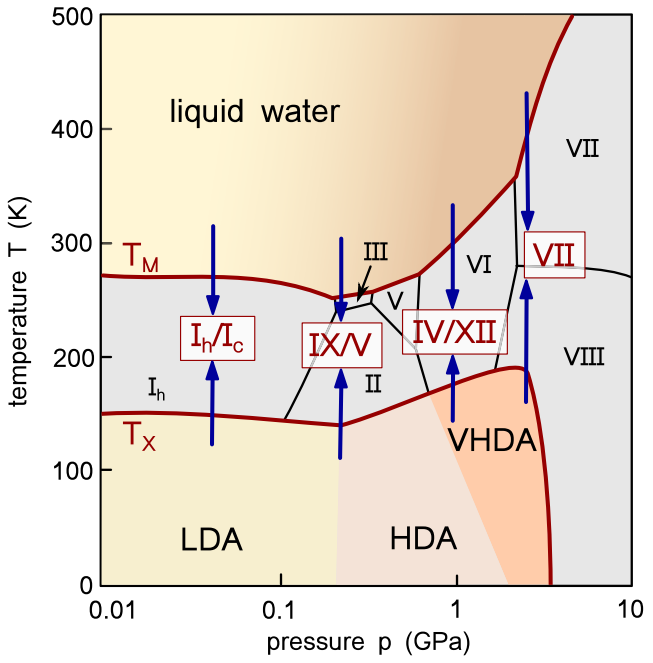

FIG. 4. The initial crystallization products of liquid water and amorphous ices. Crystallization products obtained upon cooling the stable or supercooled liquids (down arrows) or upon heating the amorphous ices (up arrows) can be identified from the boxed roman numerals appearing near the arrow heads. Stable ice phases and phase boundaries within the no man's land are marked by small roman numerals and thin lines, respectively.

supercooled liquids) are the same. Below 0.2 GPa pressurized liquid water and LDA both crystallize to cubic or hexagonal ice (Petrenko and Whitworth, 1999; Hansen, Falenty, and Kuhs, 2007). Above 0.2 GPa metastable ice III/IX or ice V crystallize from HDA and from supercooled water (Seidl *et al.*, 2013). For 0.8 to 1.9 GPa the ices IV and XII may crystallize from VHDA and from supercooled water (Loerting *et al.*, 2002; Salzmann *et al.*, 2003b; Klotz, Strässle, Saitta *et al.*, 2005). Above 2 GPa ice VII crystallizes from VHDA and from the pressurized liquid (Hemley, Chen, and Mao, 1989; Klotz *et al.*, 2003). Most interestingly, the ice phases crystallizing from amorphous ice below and from supercooled water above the no man's land often turn out as metastable, i.e., in most cases they do not correspond to the stable ice phases (small unboxed roman numerals in Fig. 4).

III. PROSPECTS FOR EXPLORATIONS WITHIN THE NO MAN'S LAND

Whether it is really permissible to link the various amorphous ices that are (meta)stable below the crystallization temperature T_X to different supercooled liquid waters envisioned for the range much above T_X is subject to the condition that for $T > T_X$ different supercooled liquid phases indeed do exist. As emphasized in the previous section, the existence of more than one (metastable) liquid water phase is not uncontested. To cast this situation into a simplified picture, Fig. 5 depicts the temperature dependent structural relaxation time τ_α together with the U shaped "nose" that reflects a characteristic crystallization time τ_x. Its numerical value specifies the time needed to form a certain fraction of ice particles of a given size and thus is not well defined but dependent on the experimental conditions. Classical nucleation theory derives the U shape by accounting for a loss of interface energy and a gain of bulk energy on the basis of opposing temperature dependences for the nucleation rates J_{ice} and the kinetically driven crystal growth rates. In other words, the liquid's shear viscosity dominates the low-temperature branch of τ_x, while its high-temperature branch is governed by J_{ice} which is small just below the thermodynamic melting point. If a temperature range exists in which the structural relaxation is longer than the crystallization time, then it is impossible to obtain an equilibrated liquid. Such a situation arises for temperatures between those denoted T_U and T_L in Fig. 5. This possibility of a "non-thermodynamic habitat" within the no man's land (see Fig. 3) was raised by Kiselev and Ely (2003). Whereas a non-thermodynamic habitat is confined within *hard* frontiers, the boundaries of the no man's land are *soft* since they are defined by the intersection of τ_x with the experimental time scale. Hence, by changing the latter, the homogeneous nucleation temperature T_H and the low-temperature crystallization temperature T_X can change as well. This should enable one to shrink the no man's land by working on shorter time scales. Conversely, τ_x, as a sample property, can be prolonged only by optimizing the sample. Considering the scenarios shown in Fig. 2, it is clear that τ_x is longer for purely glassy materials than it is for materials containing (nano)crystallites. Recent experiments by Seidl *et al.* (2015) suggest that structural relaxation and "nose" cross not just once at an upper temperature T_U as usually assumed, but again near a temperature T_L so that for $\tau_\alpha < \tau_x$ equilibrated low-temperature states are expected as well; see Fig. 5. However, with the continuity of the τ_α trace thus interrupted and possibly not even existent, questions regarding the relation of the high- and the low-temperature waters arise. Not the least, this involves the possibility that the "low-temperature water" itself is crystalline.

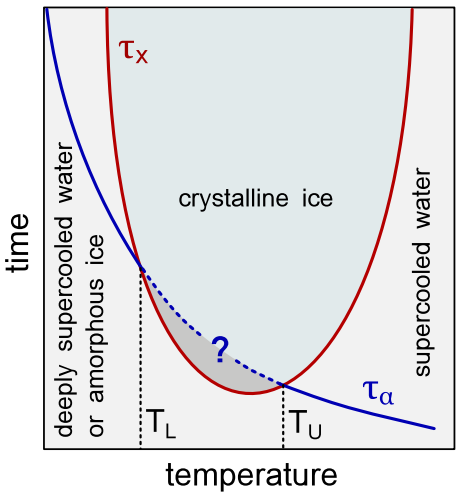

FIG. 5. The imagined relation between water's structural relaxation time τ_α and its typical crystallization time scale τ_x as it evolves below the melting temperature. Based on the classical approach of nucleation and subsequent crystal growth, the characteristic time τ_x, required to form a certain percentage of ice, is indicated by the U shaped curve. The τ_α line is drawn here to intersect the τ_x trace at an upper and a lower temperature. Designated here as T_U and T_L, respectively, these represent the hard upper and lower limits between which water crystallizes faster than it would relax or equilibrate. Complete and inevitable crystallization assumed, these limits would enclose a nonthermodynamic habitat in which τ_α cannot be defined and therefore is shown as a dotted line interrupted by a question mark.

The homogeneous crystallization of supercooled water close to T_H, of utmost relevance also for the physics of clouds in the upper atmosphere (Murray *et al.*, 2012), has been scrutinized in several recent computer simulations. Moore and Molinero (2011) found that the rate at which fourfold coordinated water molecules assemble near T_H controls the rate at which tetrahedrally structured critical ice nuclei emerge as well. Their simulations imply that below about 205 K ice nuclei form faster than the liquid can equilibrate. Using a different water model, Russo, Romano, and Tanaka (2014) identified metastable ice crystallites with tetragonal symmetry (called ice 0) which they reported to be structurally similar to the low-density supercooled liquid. This finding suggests a close-to-vanishing liquid-solid interfacial energy so that the crystalline nuclei can explosively ripen into a disordered stacking of cubic and hexagonal ice (Kuhs *et al.*, 2012; Malkin *et al.*, 2015).

The quasi-instantaneous crystallization can be monitored experimentally in aerosols cooled at rates of up to $\approx 10^7$ K/s. Some crystallization studies use liquid droplets with diameters

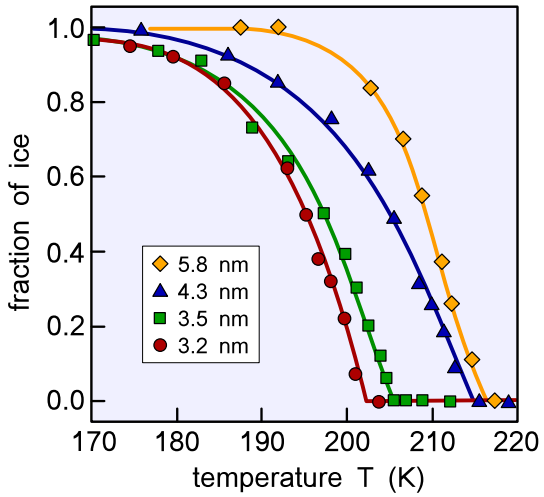

FIG. 6. Experimental determination of the fraction of crystalline ice particles for different radii of the quenched liquid droplets. The results show that the fraction increases precipitously below a threshold temperature which can be as low as ≈205 K for the smallest mean droplet radius of 3.2 nm. From Manka *et al.*, 2012.

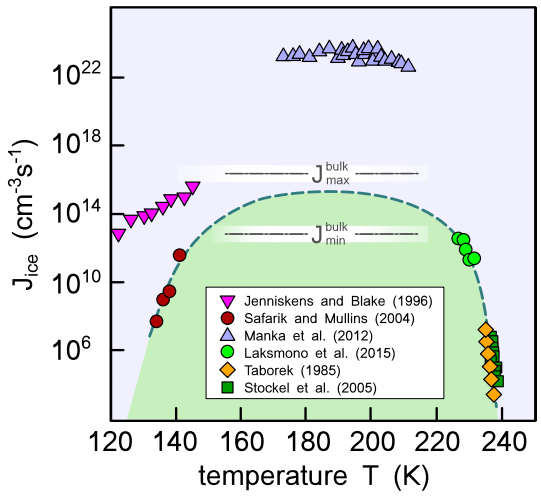

FIG. 7. Temperature dependence of experimentally determined nucleation rates J_{ice} describing the crystallization of ice from liquid droplets or amorphous films. The straight lines refer to estimates of the minimum and maximum nucleation rates within the no man's land (see footnote 4) for water droplets of 3 μm in diameter (in the figure referred to as "bulk") as employed in typical hyperquenching experiments. References to the citations listed in the inset can be found in Bhabhe, Pathak, and Wyslouzil (2013). Recent results from Laksmono *et al.* (2015) are also included.

down to a few nanometers,[3] containing only several thousand molecules (Bartell and Huang, 1994; Manka *et al.*, 2012). Figure 6 reveals that in such experiments a small fraction of the nanosized droplets remains unfrozen even far below 200 K. The number of nucleation events per volume and time, J_{ice}, can be assessed via the fraction of frozen particles typically on microsecond time scales. Near 200 K the effective nucleation rate in nanosized droplets is incredibly much larger than in micron-sized droplets near 240 K (Bhabhe, Pathak, and Wyslouzil, 2013; Ickes *et al.*, 2015) as Fig. 7 compiles.

Micron-sized droplets can be cooled through the no man's land at ultrafast rates, only: At cooling rates of 10^4 K/s all droplets still freeze, but no crystallization is detectable for droplets of 3 μm in diameter that are hyperquenched at 10^7 K/s (Kohl, Bachmann, Hallbrucker *et al.*, 2005). As indicated in Fig. 7 this finding constrains the maximum nucleation rates for bulk water.[4] If bulk water froze as fast as nanodroplets do then even cooling rates of 10^7 K/s would be insufficient to allow for vitrification of micron-sized droplets. The much faster nanodroplet crystallization evident from Fig. 7 is probably caused by the high internal Laplace pressure and/or by a switch from bulk to surface nucleation. The finding of Kohl, Bachmann, Hallbrucker *et al.* (2005) that all droplets freeze at 10^4 K/s implies that deep within the no man's land J_{ice} has to be at least 10^{13} cm^{-3} s^{-1}. The enhanced nucleation rates reported by Jenniskens and Blake (1996) (see Fig. 7) suggest that their amorphous solid water (ASW) films could have been preseeded with a small fraction of crystalline ice.

Concerning the observations that Kohl, Bachmann, Hallbrucker *et al.* (2005) made at cooling rates of 10^4 and 10^7 K/s as well as based on our estimates (see footnote 4) within the no man's land, the nucleation rate of bulk water should be confined to the band enclosed by the straight lines in Fig. 7. There a possible temperature dependence for J_{ice} is suggested (dashed line) that allows for this scenario to be consistent with most experimental findings. Note that this line is expected to describe bulk water's nucleation at $p \leq 1$ bar, but not at high pressures. Recent evaporative cooling of micron-sized droplets has allowed Laksmono *et al.* (2015) to extend measurements of J_{ice} down to 227 K; see the circles in Fig. 7. At 227 K J_{ice} has almost reached the nucleation rate J_{min}^{bulk} suggested by the dashed line in Fig. 7. Within the no man's land the temperature dependence of J_{max} is of course highly uncertain. But it is interesting to note that Moore and Molinero (2011) estimated the temperature of the maximum crystallization rate to be about 225 K.

Using femtosecond x-ray laser pulses Sellberg *et al.* (2014) examined the structure factor $S(Q)$ of water in micron-sized droplets evaporatively cooled to about 227 K, just below T_H. They found that even then a few droplets (100 out of ~3600) remained liquid on millisecond time spans and that water's strongly temperature dependent $S(Q)$ (Narten and Levy, 1971;

[3]Note that the surface tension ≈70 mN/m of water droplets with a mean radius $\langle r \rangle = 3.2$ nm generates an internal pressure of 44 MPa if the macroscopic Laplace law is applied and that the enormous surface-to-volume ratio of nanoscopic droplets enhances their surface nucleation probability substantially.

[4]At a rate of $q \approx 10^7$ K/s it takes about $\Delta t \approx 5$ μs to cool through the ~230 to ~180 K interval. Assuming that already $N = 1$ nucleation event suffices to crystallize a droplet of radius $\langle r \rangle$, one obtains $J_{max} = N/(4\pi \langle r \rangle^3 \Delta t/3) \approx 1.5 \times 10^{16}$ cm^{-3} s^{-1} for $\langle r \rangle = 1.5$ μm. This rough estimate represents a hard limit for the maximum nucleation rate of micron-sized droplets within the no man's land for bulk water at $p \leq 1$ bar. Using $q \approx 10^4$ K/s a minimum nucleation rate, $J_{min} = 1.5 \times 10^{13}$ cm^{-3} s^{-1}, is calculated analogously.

Soper, 2014) evolves smoothly toward that of low-density amorphous ice. This suggests at least *structural* continuity of the supercooled and vitrified waters that exist near the upper and the lower boundary, respectively, of the no man's land. Since hyperquenching of liquid droplets at 10^7 K/s produces LDA ice, this suggests that density fluctuations in the liquid proceed much faster than crystallization. That is, changes of density take place before crystallization emerges, thus rationalizing the initially surprising observation that supercooled and vitrified water both crystallize to the same, metastable polymorphs; see Fig. 4.

To beat water's spontaneous crystallization, small sample volumes are employed also in studies dealing with water in spatial confinement, rather than in a water vapor environment relevant for experiments with droplets. Water crystallization can be completely suppressed for instance in silica pores of only a few nanometers across (Mallamace *et al.*, 2013). However, this size corresponds to less than ten layers of water molecules with several or all of them affected by interactions with the pore walls.

Alternatively, deeply supercooled aqueous solutions were studied extensively for a wide range of solutes and dilutions (Angell, 1982; Capaccioli and Ngai, 2011; Biddle, Holten, and Anisimov, 2014). By extrapolating concentration dependent T_g measurements for solvents such as glycerol, ethylene glycol, or methanol to zero concentration, already Rasmussen and MacKenzie (1971) suggested a glass transition temperature of about 136 K for pure LDA. Nevertheless, there is a lively discussion about how much these "tricks to avoid crystallization" (Caupin, 2015) of confined waters can tell us about the static and dynamic properties of the *bulk* liquid. Although confined water studies represent a large and important research field, we favor the viewpoint that confined water, which does not freeze within milliseconds at 200 K, is different enough from bulk water. Confinement effects will not be discussed in the present context.

In addition to droplet freezing experiments, Fig. 7 includes crystallization rates obtained for amorphous ice films near 140 K. It is likely that the large deviations among the various data sets are due to different levels of (nano)crystalline contamination in the differently prepared films. In fact, efforts directed at reducing the crystallization rates are currently being undertaken not only to push the upper end of the no man's land down but also to lift its lower boundary. Seidl *et al.* (2015) emphasized that suitable sample treatment decreases the crystallization rates by orders of magnitude and hence it increases the crystallization temperature T_X of amorphous ice by at least 11 K. Furthermore, heating 150 nm thin amorphous solid water films with rates of 2.4×10^4 K/s pushes T_X even up by 25 K to about 175 K (Sepúlveda *et al.*, 2012). Studies of this type might put us closer to a position in which we can hope to address the question whether the no man's land can be brought to a (near) close.

IV. PREPARATIONS AND STRUCTURES OF AMORPHOUS ICES

A detailed understanding of the amorphous ices is impossible without knowledge about their preparation and their static structure. It has to be kept in mind, though, that due to their out-of-equilibrium nature all amorphous ices will inevitably tend to relax toward more stable states as time progresses. The key question then is whether or not this relaxation leads to fully equilibrated states: If so they are still metastable with respect to, e.g., crystalline ice, otherwise they need to be regarded as unstable.

Amorphous ices can be prepared using low- or high-pressure techniques. The latter, usually starting from crystalline ice, generate HDA or VHDA. All low-pressure routes described below produce LDA after suitable relaxation. One of them, cooling of the equilibrium *liquid*, resembles the traditional way of glass making (Kauzmann, 1948; Zarzycki, 1991). Water, by contrast to the melts used in producing window glass, is a bad glass former. That is, as for the preparation of metallic glasses (Bhat *et al.*, 2007) prior to the work in the early 1990s [see Johnson (1999) for a review], rapid quenching or clever processing is required to "beat crystallization" (Johnson *et al.*, 2011). For water, Mayer (1985) demonstrated that at cooling rates as high as 10^5 K/s crystallization and vitrification are still competing so that partially crystalline samples result. Only at 10^7 K/s, achievable, e.g., by splat cooling of micron-sized droplets, a crystal-free glassy material called hyperquenched glassy water (HGW) is obtained (Brüggeller and Mayer, 1980; Mayer and Brüggeller, 1982; Kohl, Bachmann, Hallbrucker *et al.*, 2005).

Similarly, water *vapor* can be cooled across the no man's land without crystallization because it is much easier to quench individual water molecules or small water clusters than micron-sized liquid droplets. Therefore, Burton and Oliver's (1935) deposition of amorphous ice from water vapor was the first successful laboratory route leading to what is called amorphous solid water (ASW). The morphology and phase of the ice thus formed depend on the deposition conditions (Stevenson *et al.*, 1999; Cartwright, Escribano, and Sainz-Diaz, 2008): Deposition temperatures <30 K yield highly strained material, occasionally but misleadingly called HDA (Venkatesh, Rice, and Narten, 1974; Jenniskens and Blake, 1994), that relaxes toward equilibrated LDA. A high-density nature of deposits obtained at 22 K was not confirmed (Smith *et al.*, 2003) and Baragiola (2003) surmised that the claimed high-density nature may be a result of inadvertent background gas adsorption on nanometer-thin films. At deposition temperatures <120 K a highly microporous material forms. Depending on the preparation details this porous ASW can display porosities on the order of 50% and specific surface areas of several hundred m^2/g (Mayer and Pletzer, 1987). If one heats porous ASW to temperatures >120 K its micropore network collapses and compact ASW forms, while crystallization to cubic ice is observed at $T > 150$ K (Jenniskens and Blake, 1996; Mitterdorfer *et al.*, 2014).

Detected in star forming regions, in comets, and in cold solar system objects, ASW is of major astrochemical importance (Collings *et al.*, 2005; Burke and Brown, 2010). With interstellar ices likely being porous, detailed insights into ASW's porosity under astrophysically relevant conditions bears far reaching implications for an understanding of molecular vapor exchange processes among solid and gas phases and ultimately also of planet formation.

While amorphous ice can be produced by exposing crystalline material to high-energy irradiation (Kouchi and Kuroda, 1990; Strazzulla *et al.*, 1992; Sartori, Bednar, and Dubochet, 1996), the most commonly applied means of amorphizing hexagonal ice is by subjecting it to high pressure. At 77 K hexagonal ice experiences amorphization above 1.0 GPa (Mishima, Calvert, and Whalley, 1984), resulting in HDA ice, more precisely called unannealed HDA (uHDA) (Nelmes *et al.*, 2006).[5] Upon annealing uHDA at pressures >0.8 GPa it transforms to VHDA (Loerting *et al.*, 2001), at intermediate pressures it relaxes to what is known as expanded HDA (eHDA) (Nelmes *et al.*, 2006), and at low pressures it transforms to LDA (Mishima, Calvert, and Whalley, 1985). If the mother phase is uHDA, LDA is categorized as LDA-I; if the mother phase is VHDA or eHDA, then it is called LDA-II. The very sharp HDA → LDA transformation, associated with a 25% density change, can be reversed by repressurizing LDA (Mishima, 1994; Winkel *et al.*, 2007). Mishima, Calvert, and Whalley (1985) called this HDA↔LDA transition first-order-like and Mishima and Stanley (1998a) suggested that toward higher temperatures it develops into the debated first-order liquid-liquid transition. This link between HDA and liquid water was vindicated by Mishima and Suzuki (2001) who demonstrated that HDA cannot be formed only from hexagonal ice, but also from rapidly cooled, pressurized bulk liquid water.

In the last decade, the investigation of high-pressure relaxation of amorphous ices surfaced important progress. First, Nelmes *et al.* (2006) recognized that the material undergoing the HDA → LDA transition in their experiments is eHDA, not uHDA. Winkel, Mayer, and Loerting (2011) then showed how the degree of relaxation and hence the thermal stability of eHDA can be improved further. Seidl *et al.* (2013) conjectured that uHDA contains nanocrystalline remnants of hexagonal ice [cf. Fig. 2(b)], so that annealing them away [cf. Fig. 2(a)] increases the resistance against crystallization of the glassy (eHDA) matrix. Likewise, nanocrystalline remnants surviving the uHDA → LDA transformation will reduce LDA's thermal stability: Hence, LDA-I should contain crystallization seeds, whereas LDA-II should not (Elsaesser *et al.*, 2010).

Based on their oxygen-oxygen radial distribution functions (see Fig. 8), the low-density ices ASW, HGW, and LDA are structurally almost indistinguishable from each other and hence often commonly named LDA-I. Dropping the reference to the specific preparation route is, however, justified essentially only for samples of ASW, HGW, and LDA if they are well annealed by, e.g., aging them for 90 min at 129 K (Fuentes-Landete *et al.*, 2015). Unannealed ASW with its high-energy micropore network is, by contrast, very different from unannealed LDA or from unannealed HGW.

In terms of oxygen-oxygen radial distribution functions (Fig. 8) and densities (Loerting *et al.*, 2011) one distinguishes three categories of amorphous ices: LDA, HDA, and VHDA. All of them are alike in terms of the first, but they differ significantly in the region between the first and the second coordination shells. One notices from Fig. 8 that LDA's first two shells are clearly separated, whereas in HDA one molecule from the second shell approaches the first near which it is interstitially accommodated (Finney, Hallbrucker *et al.*, 2002). In VHDA even two molecules are located in interstitial sites (Finney, Bowron *et al.*, 2002).

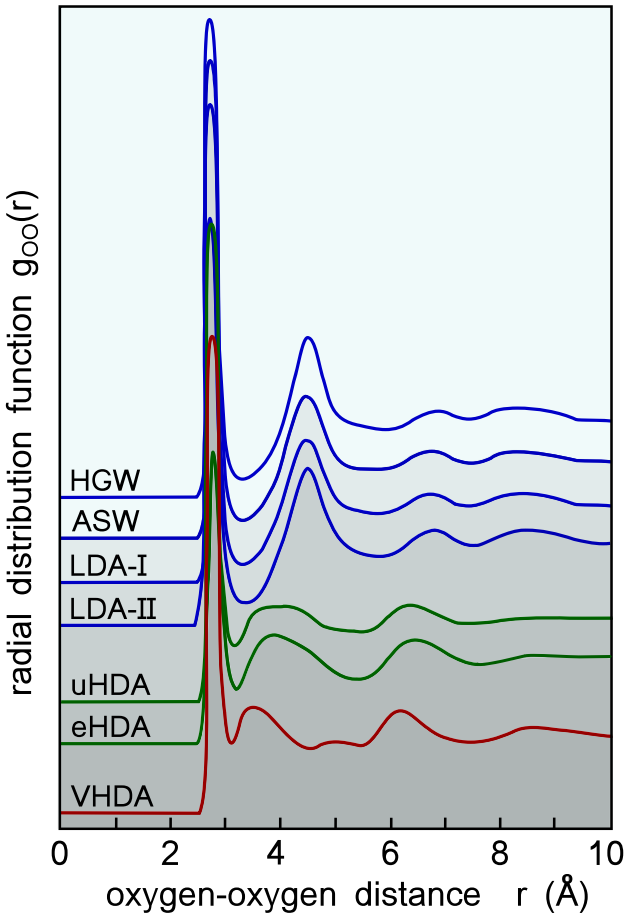

FIG. 8. Oxygen-oxygen radial distribution functions of several amorphous ices. These data are derived from empirical potential structure refinement of neutron diffraction experiments carried out for different isotopomers at a temperature of 80 K. For HGW, ASW, LDA-I, uHDA, and VHDA the results are from Bowron *et al.* (2006), for LDA-II from Winkel *et al.* (2009), and for eHDA from Loerting *et al.* (2011).

At about 0.2 GPa the Gibbs free energy of HDA equals that of LDA (Whalley, 1984; Floriano *et al.*, 1989; Whalley, Klug, and Handa, 1989) and so a reversible transition between HDA and LDA is achievable at high pressures only. By contrast, all studies at 1 bar investigate the *irreversible* transition from (V)HDA to LDA, i.e., a transformation driven by a Gibbs free energy difference which is kinetic rather than thermodynamic in origin. Consequently, at ambient pressure unstable intermediate amorphous states also become observable in the course of the transition (Tulk *et al.*, 2002). These states, called intermediate density amorphous ice by Urquidi *et al.* (2004) or HDA' by Koza (2009), cannot be equilibrated and, as such, cannot be proxies of supercooled liquids. By contrast one may wonder: Could LDA, HDA, and VHDA possibly be proxies of supercooled liquids? This question is addressed next.

[5]Here and in the following we refer to the amorphous ices in terms of today's more specific, yet unsystematic nomenclature irrespective of whether or not this designation was used in the cited publications.

V. HOW DO AMORPHOUS ICES THAW?

This section aims at collecting some of the arguments put forward on the basis of laboratory experiments to support the idea that amorphous ices above their glass transition are to be regarded either (i) as supercooled liquids characterized by translational *and* orientational disorder or (ii) as crystalline states characterized by only orientational disorder. A variety of experimental methods were employed in order to study water's controversial glass transitions. Within the compass of this Colloquium, in the following sections we mostly focus on calorimetry, x-ray and neutron techniques, as well as on dielectric relaxation and nuclear magnetic resonance, i.e., on methods applied by our and other research groups. However, results from many other experimental methods will be discussed as well. These include thermal desorption (Smith and Kay, 1999), vibrational spectroscopy (Fisher and Devlin, 1995) and combinations thereof (Moon *et al.*, 2012), as well as thermal conductivity (Johari and Andersson, 2007) and mechanical testing (Johari, 1998). This list of references which does not feature, e.g., hydroxyl stretching vibration studies of neat amorphous ices (Shalit, Perakis, and Hamm, 2013; Tainter, Shi, and Skinner, 2014; Parmentier *et al.*, 2015) is obviously neither representative nor exhaustive.

A. Calorimetric and transport studies

Whether or not amorphous ices below the low-temperature crystallization temperature T_X are thermodynamically continuously connected with the supercooled liquid above the homogeneous nucleation temperature T_H cannot be answered at present because of the restrictions imposed by rapid crystallization occurring within the no man's land. Nevertheless, attempts were made at answering the question of thermodynamic continuity, e.g., based on simulation methods typically addressing the nanosecond time scale. While in some simulations a discontinuity between LDA and supercooled water was inferred at ambient pressure (Shpakov *et al.*, 2002), others saw a continuous connection (Poole *et al.*, 1992; Sastry *et al.*, 1996; Rebelo, Debenedetti, and Sastry, 1998; Ponyatovsky and Sinitsyn, 1999). Experiments on nanosecond time scales are yet to be carried out, and so numerous laboratory studies focus on the temperature region just below T_X. Here, the main, controversially debated question has focused on whether or not amorphous ices experience a glass-to-liquid transition at $T_g < T_X$. If so, amorphous ices are thermodynamically continuously linked with deeply supercooled liquid water. It is then often tacitly assumed that in turn there has to be a continuous thermodynamic connection between deeply supercooled water below T_X and supercooled water above T_H.

For a long time the question regarding the nature of the glass transition in amorphous ices focused on LDA-type ices at ambient pressure. McMillan and Los (1965) first reported the glass transformation in ASW to occur at 139 K. Similar glass transition onset temperatures of (136 ± 1) K were observed for well-annealed ASW (Hallbrucker, Mayer, and Johari, 1989a), HGW (Johari, Hallbrucker, and Mayer, 1987; Hallbrucker, Mayer, and Johari, 1989b), and LDA ices (Johari, Hallbrucker, and Mayer, 1991; Elsaesser *et al.*, 2010); see the curves in Fig. 9. In all of these studies an increase of $\Delta C_p \sim 1\ \mathrm{J\,K^{-1}\,mol^{-1}}$ was found in heat capacity measurements. It has to be noted, though, that the end point of the glass transition cannot be detected in full because the incipient crystallization to cubic ice intervenes. Judging from the width of water's calorimetric glass transition it seems that its end point is almost reached in the experiments by Hallbrucker, Mayer, and Johari (1989b). Also heating- and cooling-rate dependent measurements suggest that they record a C_p overshoot just prior to the end point (Kohl, Bachmann, Hallbrucker *et al.*, 2005; Kohl, Bachmann, Mayer *et al.*, 2005), implying that LDA's glass transition is very feeble and associated with a small heat capacity increase. These findings suggest that deeply supercooled liquid water might be a strong or even superstrong liquid (Angell, Moynihan, and Hemmati,

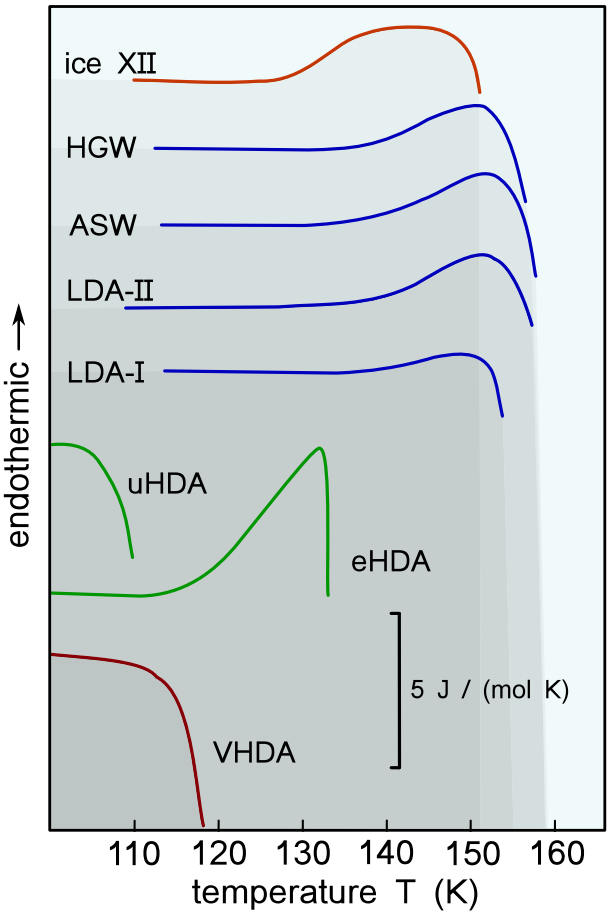

FIG. 9. Heat capacity changes recorded for various amorphous ices after suitable annealing. For comparison, the differential scanning calorimetry curve of crystalline ice XII, which can be considered an orientational glass, is also shown. The exothermic downturns stem from the incipient transformation of the samples to cubic ice (from ice XII, HGW, ASW, LDA-I, and LDA-II) or to LDA (from uHDA, eHDA, and VHDA). The eHDA trace was recorded at a heating rate of 10 K/ min, all others at 30 K/ min. Data for HGW are from Johari, Hallbrucker, and Mayer (1987), for ASW from Hallbrucker, Mayer, and Johari (1989a), for LDA-I and ice XII from Salzmann *et al.* (2003a), for uHDA and VHDA from Loerting *et al.* (2011), and for eHDA and LDA-II from Amann-Winkel *et al.* (2013).

2000), if the glass transition indeed connects LDA with a liquid state.

Based on infrared spectroscopic measurements, Fisher and Devlin (1995) doubted, however, that amorphous ice is connected to a liquid state. By photoexcitation of 2-naphtol they injected excess protons into amorphous ice containing a few isolated D_2O molecules and studied the resulting H/D isotope exchange dynamics. According to their measurements the protons thus injected at 80 K travel only short distances and they form some decoupled $(HOD)_2$ units. Furthermore, Fisher and Devlin (1995) concluded that the protons follow the dynamics expected for an icelike point defect model. They rationalize their observations at 125 K, still below the calorimetric T_g, in terms of a beginning orientational defect activity based diffusion and they rule out relevance of molecular transport and fluidity when warming ASW to beyond 130 K. Overall, Fisher and Devlin (1995) implied that the dynamics in ASW is similar to that in cubic ice. From a comparison of the heat capacity increase observed for LDA with that for orientational ice glasses also Shephard, Evans, and Salzmann (2013) suggested orientational diffusion, but not translational diffusion to occur at the glass transition. That is, they suggested a transformation from one glassy state, in which all atoms are immobile, to yet another glassy state in which hydrogen atoms are mobile whereas the oxygens are not. To illustrate their point Fig. 9 shows the heat flow through samples, e.g., of LDA and of ice XII. These calorimetry traces display the same qualitative features, i.e., an increase in heat capacity of about 1 $J\,K^{-1}\,mol^{-1}$ near 130 K, followed by a latent heat release when the sample transforms to ice I_c. However, calorimetry traces alone do not allow one to judge whether or not translational mobility is involved at a glass transition. Clearly, at the orientational glass transition of ice XII the oxygen atoms do remain at their lattice positions, but this may or may not be so at the glass transition of the amorphous ices.

Strong arguments for a fluid nature of the oxygen network were advanced by others: The activation energy of 55 kJ/mol characterizing the presumed structural relaxation reflects the energy required to break two hydrogen bonds (Hallbrucker, Mayer, and Johari, 1989b). The breaking of two hydrogen bonds allows for translation diffusion, whereas proton-jump diffusion implies the creation of point defects; their generation requires larger and their migration much smaller activation energies than 55 kJ/mol. Then, Johari (1998) observed softening and blunt indentor penetration of LDA when warming it to 140 K. Finally, from a study of the proton-deuteron intermixing in thin ASW films Smith and Kay (1999) concluded that the magnitude and temperature dependence of the diffusivity at 150 K is consistent with the idea that ASW thaws into a metastable extension of deeply supercooled water.

The controversy centering on the interpretation of the heat capacity increase in calorimetry experiments and the question whether or not translational motion is indicated from isotope exchange measurements has not yet been resolved. Other suggestions concerning the increase in heat capacity at 136 K have included that it might be a shadow of a real glass transition (Yue, Jensen, and Christiansen, 2002; Giovambattista *et al.*, 2004) at 165 K, so that T_g would be larger than T_X. In view of further experiments (Kohl, Bachmann, Hallbrucker *et al.*, 2005; Kohl, Bachmann, Mayer *et al.*, 2005), the glass transition has been reaffirmed to take place at 136 K (Angell, 2007), provided that water is not a fragile liquid near T_g (McClure *et al.*, 2006). Overall, the question regarding the nature of the molecular motions activated near T_g, and hence the thermodynamic connection of LDA with the deeply supercooled liquid, remains controversial.

Only recently was the discussion extended from the low- to the high-density amorphous ices. Loerting *et al.* (2015) reviewed the current state of experiments related to HDA and VHDA at pressures up to 2 GPa. In brief, glass transitions were found for HDA and VHDA using *in situ* high-pressure methods for $p > 0.2$ GPa, at which HDA and VHDA are more stable than LDA. Experiments included measurements of VHDA's heat capacity at 1 GPa (Andersson, 2011), thermal effects in pure HDA at 0.5 GPa (Mishima, 2004), vitrification of emulsified liquid water at 0.5 GPa (Mishima and Suzuki, 2001), observation of volumetric glass transitions in isobaric heating experiments of HDA up to 0.3 GPa (Seidl *et al.*, 2011), and extrapolation of structural relaxation times of HDA at 0.2 GPa obtained from isobaric and isothermal annealing studies (Handle, Seidl, and Loerting, 2012). Because of the slow conversion kinetics of eHDA to LDA the glass transition of HDA could also be found below 0.2 GPa, i.e., in a region in which eHDA is metastable with respect to LDA. The experiments by Seidl *et al.* (2011) and Handle, Seidl, and Loerting (2012) indicated a continuous trend of HDA's glass transition temperature also for pressures below 0.1 GPa. These results demonstrated that metastability alone does not preclude the observability of glass transitions, if the precondition is met in which the time scale of transformation is much longer than the time scale of equilibration.

The transformation time scales can considerably exceed those required for the equilibration also of eHDA, at least at ambient pressure. Therefore, measurements of eHDA became possible in an extended temperature range and revealed an ambient-pressure heat capacity step at 116 K (Amann-Winkel *et al.*, 2013). By contrast, the precondition defined above is not met for uHDA which was the only form of HDA studied in the 20th century. uHDA transforms to LDA at ~110 K, long before equilibration of the amorphous matrix is possible (Handa, Mishima, and Whalley, 1986; Loerting *et al.*, 2011), and so the increase in heat capacity, marking HDA's glass transition at 116 K, cannot be observed for uHDA; see the uHDA curve in Fig. 9. Similarly, at 1 bar VHDA also transforms first to LDA before a glass transition can be reached; see the VHDA curve in Fig. 9. The pressure dependence of T_g for HDA and VHDA samples was recently reported by Handle and Loerting (2016). Most notably, T_g increases with pressure up to 160 K at 0.7 GPa and then suddenly drops by about 30 K (see Fig. 3), which indicates significantly faster hydrogen bond dynamics in VHDA than in HDA.

B. Wide- and small-angle diffraction: Structural homogeneity and heterogeneity

Structural studies of amorphous ices were directly linked to the quest of preparing amorphous ices. Early x-ray and neutron wide-angle diffraction on ASW (Dowell and

Rinfret, 1960; Venkatesh, Rice, and Narten, 1974), HGW (Hallbrucker *et al.*, 1991; Bellissent-Funel *et al.*, 1992), and uHDA (Floriano *et al.*, 1986; Bizid *et al.*, 1987) helped in clarifying that the amorphous ices can be understood in terms of structural models developed for liquid water. The most comprehensive set of data was collected by Finney and coworkers (Finney, Bowron *et al.*, 2002; Finney, Hallbrucker *et al.*, 2002; Bowron *et al.*, 2006; Winkel *et al.*, 2009; Loerting *et al.*, 2011) using neutron diffraction on ASW, HGW, LDA-I, LDA-II, uHDA, eHDA, and VHDA; see the oxygen-oxygen radial distribution functions compiled in Fig. 8. The results of all these studies are consistent with the idea that the amorphous ices are structurally homogeneous. However, while none of these studies detected crystalline contaminations, this does not rule out the presence of (sub)nanometer sized crystallites since wide-angle scattering is unable to discriminate the scenarios depicted in Fig. 2.

By contrast, wide- and small-angle neutron scattering results by Koza and colleagues [see Koza (2009), and references cited therein] showed that uHDA is structurally heterogeneous on the nanometer scale. According to Koza and colleagues the first diffraction peak of the momentum transfer dependent static structure factor $S(Q)$ is much broader for uHDA than it is for VHDA or for LDA-I. Furthermore, they reported that uHDA displays a much stronger low-Q ($Q < 0.3$ Å^{-1}) scattering intensity than the structurally homogenous LDA-I and VHDA ices. They concluded that only VHDA and LDA-I, but not uHDA, should be considered as glassy counterparts of the high-density and low-density liquids, and they substantiated these results by tracking the time dependent structure factor $S(Q)$. By carrying out these experiments isothermally at ambient pressure, the VHDA → LDA transformation was monitored. The intermediate states formed during the transformation display the same heterogeneity as uHDA but their structure factor cannot be reproduced by superposing the homogeneous VHDA and LDA-I structures. This failure to observe a first-order-like transition makes sense at ambient pressure at which an equality of the Gibbs free energies does not exist; cf. Sec. IV. A first-order-like HDA↔LDA transformation is, however, expected in the presence of such an equality. Indeed, experiments by Nelmes *et al.* (2006) and Winkel, Mayer, and Loerting (2011) indicated that a first-order-like transition between eHDA and LDA-II takes place at pressures near 0.07 GPa. Upon decompressing pressurized eHDA at 140 K, Winkel, Mayer, and Loerting (2011) observed spontaneous formation of an interface between eHDA and LDA-II and its subsequent propagation through the sample. The x-ray diffractogram of the interface region could be represented as a superposition of eHDA and LDA-II patterns. In the course of the transformation two superposed halo peaks were observed instead of a single one, i.e., the position of the halo maximum does not evolve continuously but it jumps from the eHDA to the LDA position. In several experiments, the interface was observed to travel from the bottom to the top and from the top to the bottom with similar probability; in some runs even two phase boundaries formed. This rules out the possibility that pressure and/or temperature gradients cause these findings. The conclusions drawn by Winkel, Mayer, and Loerting (2011) from their *ex situ* study of the HDA → LDA transition are complementary to analogous results based on Klotz, Strässle, Nelmes *et al.*'s (2005) *in situ* neutron diffraction work regarding the LDA → HDA transition.

While these studies make a strong case for a first-order-like eHDA↔LDA transition at elevated pressure, important experiments remain to be done to resolve persisting issues: The similarity of eHDA's and uHDA's first diffraction peak (Loerting *et al.*, 2011) suggests that also eHDA is structurally heterogeneous, but small-angle scattering data for eHDA are needed to test this conjecture. Furthermore, an elucidation of the nature of the LDA↔HDA and the LDL↔HDL transitions requires further *in situ* studies at pressures near 0.2 GPa and near T_X, in particular, also of the *dynamical* properties of various amorphous ices.

C. Slow dynamics: Dielectric spectroscopy and magnetic resonance

Apart from the experiments dealt with in Sec. V.A, the slow dynamics of the amorphous ices can be monitored using dielectric and nuclear magnetic resonance (NMR) spectroscopy that allow one to determine the time scales (and their possible distribution) on which the orientations of the water molecules fluctuate. While these techniques were extensively exploited to study crystalline ices [see Petrenko and Whitworth (1999) for a comprehensive reference list], NMR was only rarely applied to *amorphous* ices. Dielectric investigations appear to be more popular and a summary of pending work performed up to 2007 is available (Johari and Andersson, 2007). Hence, focusing on results obtained for amorphous ices in the last decade we discuss properties such as (1) the spectral shape of the dielectric spectra, (2) dynamics probed by temperature and pressure dependent studies, (3) transformation kinetics among different states, as well as (4) influence of impurity doping.

1. Spectral shape

Generally, dielectric loss spectra are peaked at frequencies which correspond to the rate τ^{-1} of molecular reorientation. As an example Fig. 10(a) summarizes loss spectra recorded for LDA-II at several temperatures and Fig. 11 shows the relaxation times determined thereof. The proton dynamics in the *crystalline* ice phases I_h, III, V, VI, and VII (Wilson *et al.*, 1965; Johari and Whalley, 1981) yields dielectric absorption peaks which, on their high-frequency side, are characterized by a power law $\varepsilon'' \propto \nu^{-\gamma}$ with an exponent γ close to 1; see Fig. 10(b) for data on ice I_h. Exponents $\gamma < 1$ indicate a distribution of underlying relaxation rates. The dielectric loss spectra of eHDA recorded at elevated and at ambient pressure reveal $\gamma \approx 0.5$; see also Fig. 10(b). This behavior resembles that of supercooled liquids where an exponent $\gamma \approx 0.5$ "appears to be a generic property of the[ir] relaxation" (Nielsen *et al.*, 2009). To enable a direct comparison of eHDA with a typical glass former Fig. 10(b) comprises a loss spectrum of glycerol. Both materials exhibit a high-frequency "excess wing" in addition to the main peak. Furthermore, in Fig. 10(b) the spectrum for LDA-II displays a near-to-peak exponent of $\gamma \approx 0.8$ which is close to that of ice I_h. However, for frequencies above 100 Hz a shoulder in the dielectric loss of LDA-II suggests the presence of a secondary relaxation. Named after Johari and Goldstein (1970) this feature is

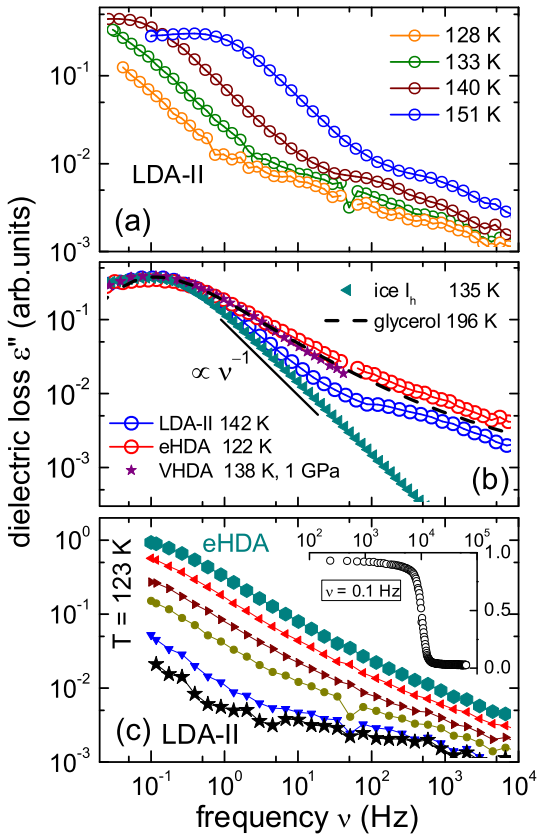

FIG. 10. (a) Dielectric loss spectra of LDA-II from Amann-Winkel *et al.*, 2013. Dipolar relaxation times can be determined from the inverse of the angular frequency at which these spectra are peaked. (b) Comparison of spectra measured for eHDA, and LDA-II [data for both samples from Amann-Winkel *et al.* (2013)] and glycerol (Kudlik *et al.*, 1999), with those of ice I_h (measured for the present work) and VHDA. The latter data are from Andersson and Inaba (2006) who renamed VHDA as rHDA. All data, except those for VHDA, were recorded at ambient pressure. The spectra are normalized to their peak amplitudes. For ice I_h the near-to-peak power-law exponent is $\gamma \approx 1$, while for HDA it is $\gamma \approx 0.5$. (c) Dielectric loss spectra are shown for annealing times of 4, 160, 176, 204, 225, and 1066 minutes after warming an eHDA sample from 77 to 123 K. These data allow one to monitor the eHDA → LDA-II transformation at a constant temperature of 123 K. The inset displays the explicit time dependence of ε'' recorded at a frequency of 0.1 Hz (Lemke *et al.*, 2014).

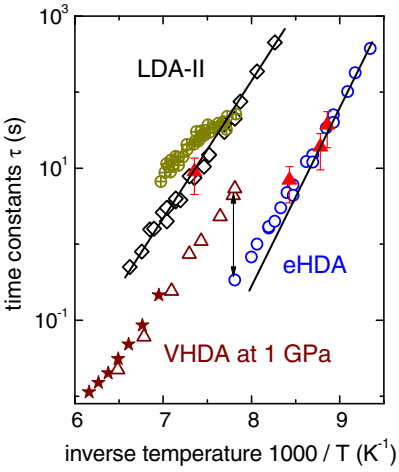

FIG. 11. Arrhenius diagram of calorimetric (filled triangles) and dielectric time constants obtained for eHDA (open circles) and for LDA-II (open diamonds) at ambient pressure (Amann-Winkel *et al.*, 2013). The VHDA data (undoped, open triangles; KOH doped, filled stars) were recorded at 1 GPa by Andersson (2005, 2008). The lines represent Arrhenius laws and the arrow at 125 K illustrates the compression induced increase of τ for the high-density amorphs. Time constants for LDA from stimulated-echo NMR are represented by crossed circles (Löw, Amann-Winkel, Loerting *et al.*, 2013).

considered generic for glass forming materials and was discussed to occur also for ASW and HGW (Johari, 2005).

2. Temperature and pressure dependent time constants

Time constants from several experimental techniques are compiled in Fig. 11: The dielectric relaxation times agree with those from calorimetry (Amann-Winkel *et al.*, 2013) and for LDA-II they are similar to the correlation times from stimulated-echo deuteron NMR (Löw, Amann-Winkel, Loerting *et al.*, 2013). The data in Fig. 11 hint at the existence of a glass transition in the amorphous ices. However, since echo NMR and dielectric spectroscopy are sensitive only to reorientational motion, the experimental results, by themselves, do not rule out other scenarios, for instance, Bjerrum defect dynamics as seen in crystalline ice I_h (Geil, Kirschgen, and Fujara, 2005).

Dynamics on nanosecond time scales dominate measurements of spin-lattice relaxation times T_1, which enable one to distinguish different amorphous ices on a phenomenological basis (Ripmeester, Ratcliffe, and Klug, 1992). More recently, Scheuermann *et al.* (2006) determined deuteron T_1 times of uHDA and of LDA-I, the latter obtained by heating the uHDA samples above their transformation temperature. Different thermal treatments lead to significant T_1 variations for uHDA and to less pronounced ones for the LDA-I specimens produced thereof. Löw, Amann-Winkel, Geil *et al.* (2013) found that near 100 K the deuteron T_1 times of several amorphous ices evolve from short to long in the following order: VHDA, uHDA, eHDA, HGW, and LDA-II; all spin-lattice relaxation times differed significantly from each other except those of the low-density variants LDA-II and HGW which display very similar T_1 times.

We now discuss the temperature dependence of the dielectric relaxation times in terms of the fragility or steepness index $m = E_{\mathrm{eff}}(T_g)/T_g$ (Böhmer *et al.*, 1993), i.e., the ratio of effective energy barrier $E_{\mathrm{eff}}(T_g)$, here in temperature units, and T_g, here defined as the temperature at which $\tau = 100$ s. With $E_{\mathrm{eff}}(T_g)$ represented by the solid lines in Fig. 11, Amann-Winkel *et al.* (2013) found that m is around 19 for eHDA and 14 for LDA-II, much smaller than values typical for van der Waals liquids, but close to those of several orientational glasses (Götz *et al.*, 2014), and of tetrahedrally bonded network liquids like SiO_2. In fact, the fragility index for LDA-II, $m = 14$, is the smallest among all glass formers and indicates "superstrong" relaxation dynamics (Angell, Moynihan, and Hemmati, 2000), a finding recently rationalized in terms of quantum effects (Novikov and Sokolov, 2013; Gainaru *et al.*, 2014).

As a function of pressure p, the dielectric time constants of many supercooled liquids obey the empirical relation $\tau(T,p)/\tau(T,0) = \exp(p\Delta V/RT)$ with ΔV denoting the activation volume (Roland *et al.*, 2005). For an approximate determination of ΔV, the dielectric relaxation times measured for VHDA at $p = 1$ GPa by Andersson and Inaba (2006) are compared with the ambient-pressure data of Amann-Winkel *et al.* (2013). Evaluated at $T = 125$ K (cf. the arrow in Fig. 11) this yields a ΔV that is close to the volume given by the geometrical diameter of the water molecule. However, since similar activation volumes were reported for several crystalline ices as well (Wilson *et al.*, 1965), ΔV is not suitable to probe the nature of the glass transition in the amorphous ices.

3. Transformation kinetics

Dielectric spectroscopy allows one to track the kinetics of transitions among different amorphous and crystalline ices relatively easily. Amann-Winkel *et al.* (2013) reported that LDA and HDA can be kept at temperatures below and even slightly above their calorimetric glass transition for long times. If, however, these temperatures are considerably exceeded, the dipolar dynamics becomes fast enough, hence τ small enough, so that the transformations toward the more stable states (i.e., from HDA to LDA and from LDA to cubic ice) can be tracked experimentally. As an example dielectric spectra recorded for eHDA at 123 K and different waiting times are presented in Fig. 10(c). The decrease in the loss amplitude shown in the inset of that figure indicates an HDA → LDA transformation time of $\approx 10^4$ s. This is about 10^4 times longer than the dipolar relaxation time of eHDA at 123 K with the separation of the two time scales rapidly increasing upon cooling. Similarly, at the LDA → ice I_c transition the transformation kinetics is also $\sim 10^4$ times slower than the dipolar relaxation of the parent state. The present results seem to differ from the inference made by Shephard, Evans, and Salzmann (2013). They found it difficult to reconcile their "findings with the postulated glass transition of LDA to the supercooled liquid before the onset of crystallization."

4. Influence of doping

Dynamics was also studied in amorphous ices containing doping-induced defects. Typical dopants are relatively small molecules that are soluble in ice in minute amounts. The HDA dynamics is insensitive to potassium hydroxide (KOH) doping, as inferred from Andersson and Inaba's (2006) high-pressure measurements; cf. Fig. 11. The calorimetric measurements of Johari, Hallbrucker, and Mayer (1991) indicated that also NH_3 and NH_4F doping leaves LDA's glass transition unaltered, although doping generally enhances proton mobility in crystalline ices significantly (Petrenko and Whitworth, 1999). An insensitivity of the LDA dynamics to impurity doping is thus to be contrasted with the scenario advocated by Fisher and Devlin (1995) which implicitly requires that suitable doping of LDA should markedly speed up the dynamics with respect to that of the nominally pure substance.

We point out that impurities, added in minute amounts to most supercooled liquids, will mainly increase their electrical conductivity rather than significantly altering their viscosity or structural relaxation time. So if, as a consequence of impurity doping, one does not observe a change of phenomena related to dielectric main peaks (such as arising, e.g., from structural relaxation) or to the calorimetric signature at the glass transition, this suggests that one deals with a liquid. Conversely, for suitably impurity doped crystalline ices one will typically observe major *changes* of the dominant dielectric relaxation (Salzmann *et al.*, 2011). In this respect, the dielectric results of KOH doped HDA and LDA indicate that these thawed amorphous ices might behave as liquids rather than as solids.

D. Collective vibrations probed by inelastic x-ray scattering

Substantial arguments questioning the glassy nature of some amorphous ices stem from inelastic x-ray scattering. Using highly monochromatic radiation, this technique allows one to track the energies $E(Q)$ that reflect the dispersion relation of the longitudinal acoustic phonons in a kinematic range not accessible to neutrons. Here the range of momentum transfers from $Q = 1$ to ≈ 7 nm^{-1} is of particular interest since with increasing Q the corresponding phonon wavelengths approach the scale of intermolecular distances. A couple of inelastic x-ray scattering experiments on amorphous ices (LDA-I: Schober *et al.*, 2000, uHDA: Schober *et al.*, 2000; Koza *et al.*, 2004, and VHDA: Koza *et al.*, 2008) yielded phonon dispersion curves reminiscent of crystalline behavior. This statement is illustrated in the upper part of Fig. 12 which compares Q dependent Brillouin lines of LDA-I and crystalline cubic ice with those of the molecular glass ortho-terphenyl. In all glasses studied so far, the longitudinal acoustic phonon branch strongly broadens with increasing momentum transfer and overdamped phonon peaks occur at relatively small Q [for a review, see Ruocco and Sette (2001)]; cf. the lower part of Fig. 12. By contrast, the phonon peaks of the amorphous ices remain almost as sharp as in crystalline ice I_c.

At first glance, this finding appears surprising because the oxygen-oxygen radial distribution function (see Fig. 8) and the static structure factor of LDA-I closely resemble those of LDA-II: both are characteristic for glasses. To appreciate this resemblance one should keep in mind that the static structure factor reflects the distribution of the minima of the interatomic potentials while acoustic phonon energies are determined by their *second derivative*. This circumstance suggests that inelastic x-ray scattering may be sensitive enough to distinguish homogeneous glassy from some kind of nanocrystalline states (cf. Fig. 2), while such differences may not easily be resolved in the static structure factor. LDA-I is indeed expected to contain a significant fraction of nanocrystalline ice (see Sec. V.A), which could rationalize the findings of Schober *et al.* (2000). So, with today's knowledge that LDA-II is structurally more homogenous than LDA-I, it is evident that corresponding inelastic x-ray scattering experiments are necessary also for LDA-II. The situation for HDA is analogous to that for LDA: Schober *et al.* (2000) and Koza *et al.* (2004) found that the acoustic phonons in uHDA, albeit somewhat broader than those of LDA-I, are still rather crystal-like. The broadening of the phonons in uHDA may be related to the pronounced heterogeneous character of this unrelaxed amorphous ice as discussed in Sec. V.B. So, inelastic x-ray

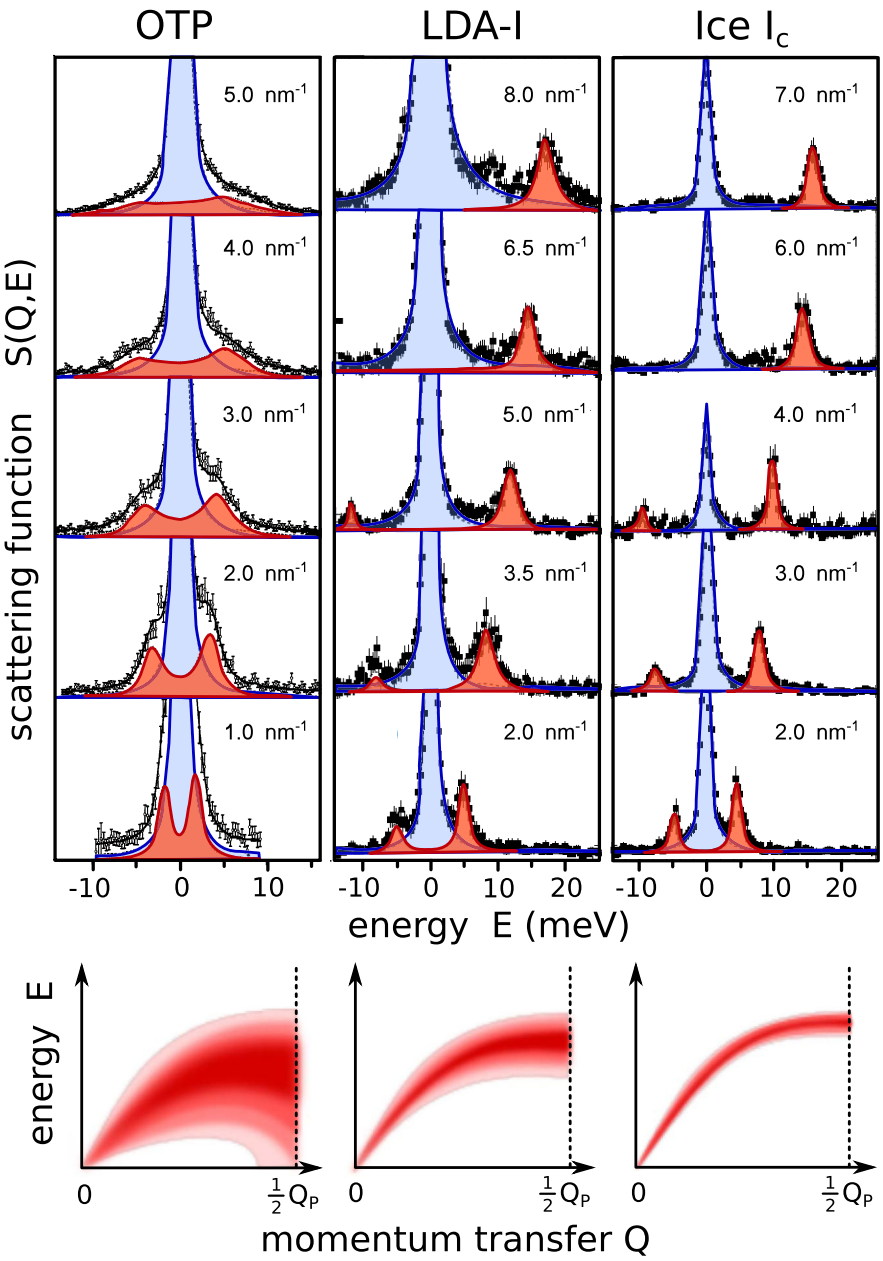

FIG. 12. Upper part: Q dependent inelastic x-ray scattering results for the molecular glass former orthoterphenyl (OTP) measured at 156 K (Monaco *et al.*, 1998) as well as for LDA-I at 60 K, and for cubic ice I_c at 80 K (Schober *et al.*, 2000). Fits to the inelastic contributions are highlighted. Lower part: Sketch of the longitudinal acoustic phonon branch for each of the three glasses with emphasis on the difference in the Q dependent width. The momentum transfer $Q_p/2$ is occasionally taken to define the edge of the first pseudo Brillouin zone. In a glass, the position of the first peak in the static structure factor $S(Q)$ is denoted by Q_p which is $Q_p = 14$ nm^{-1} for orthoterphenyl and 16 nm^{-1} for LDA-I and for ice I_c. Note that in a crystal the branch remains relatively narrow while in a glass a strong overdamping broadens the phonon peaks considerably as Q increases. LDA-I rather resembles the behavior of crystalline ice I_c.

scattering experiments should be performed for eHDA which appears to be free from nanocrystallites and should be structurally homogeneous as well.

Also inelastic *neutron* scattering was exploited to study phonon branches and phonon density of states of several amorphous ices. However, Koza (2008) pointed out that for kinematic reasons neutron scattering traces phonons only in the second and higher pseudo Brillouin zones. In those the acoustic and optical phonon branches mix and the interpretation of such neutron spectra [see also, e.g., Li and Jenniskens (1997) and Kolesnikov *et al.* (1999)] gets more involved and less conclusive with respect to the nature of collective vibrational excitations. Interestingly, numerical simulations of amorphous ice networks by Belosludov *et al.* (2008) found evidence for well-defined phonon branches. Further work should aim at delineating the microscopic origin of this seeming discrepancy: How can crystal-like phonons exist in amorphous structures?

VI. ASSESSMENT OF EXPERIMENTAL RESULTS AND PERSPECTIVES

Stunningly, several experimental observations raise the possibility of a feeble glass-to-liquid transition in amorphous ices. In fact, up to three distinct glass-to-liquid transition temperatures and hence the occurrence of multiple (deeply supercooled) liquid states of the single-component system H_2O has been suggested; see Fig. 3.

Furthermore, the likely existence of liquid water down to temperatures as low as 116 K sounds amazing. But, as mentioned previously, many questions regarding the nature of the molecular motions above the glass transition and the vibrational properties of the amorphous ices remain and we can only hope that their resolution will not take too long. At this point it is worthwhile, however, to recall that despite intensive research effort, an at least 20-year long debate has centered on clarifying the structural diversity or similarity and even identity of various amorphous ices. Careful x-ray and comprehensive neutron scattering experiments involving detailed analyses together with refined sample preparation protocols resolved many issues in this context. Today, most workers consider the differently produced low-density amorphous ices (ASW, HGW, LDA) structurally identical, provided they are appropriately annealed. While it is also well established that three forms of amorphous ice (LDA, HDA, and VHDA) need to be properly distinguished, the relation between and the nature of the transitions among them is still not fully clarified. At present, it seems that the LDA-HDA transition is first-order-like, whereas the HDA-VHDA transition displays a broader, weakly discontinuous, or continuous nature.

Partly based on the thorough investigations of unannealed samples by Koza and others, as reviewed in Sec. V.B, agreement regarding HDA is not complete (Limmer and Chandler, 2014). The conclusion drawn from the small-angle scattering studies was that uHDA is not a well-defined amorph but merely a state characterized by frozen-in heterogeneities. However, evidence is growing that without proper annealing (nano)crystalline remnants exist in such samples. Hence, to fully elucidate the nature of these heterogeneities elastic scattering experiments on well-annealed eHDA samples are needed. Well-annealed samples are metastable and presumably homogeneous, so that only they could be low-temperature proxies of liquids. In the same vein, the experiments discussed in Sec. V.D, which provide strong support for a (nano)crystalline origin of the relatively sharp phonon bands in unannealed samples, should be extended to eHDA and likewise to LDA-II. We conjecture that these amorphous ices, like annealed HGW and annealed ASW, will display more glasslike phonon behavior, but they are yet to be studied using inelastic x-ray scattering experiments. So, in the end, much of the perceived controversy may boil down to comparing apples and oranges, where the amorphous ices LDA-I and uHDA belong to one category [cf. Fig. 2(b)], and the amorphous ices LDA-II, eHDA, and VHDA to another [cf. Fig. 2(a)].

The situation is not entirely straightforward when considering investigations of slow dynamics. The milestone experiments on the low-density amorphous ices [cf. Sec. V.A, by Fisher and Devlin (1995)], rejecting the notion that fluidity is accompanying the dynamic unfreezing, as well as those by Johari (1998) and Smith and Kay (1999) both interpreted in terms of a liquid-to-glass transition, were all performed a while ago. But no one has succeeded in proposing a generally accepted way out of this seeming dilemma and hence, as experimentalists, we feel that we should resort to additional laboratory studies.

The key question, to us, remains whether above the glass transition the water molecules display liquid-like bulk fluidity or not. Some researchers are concerned that in order to rationalize Johari's (1998) indentor experiments on LDA-I macroscopic plasticity rather than microscopic mobility is sufficient, although it is hard to see how the former can arise without the latter. Future experiments should determine the shear viscosity of, e.g., LDA-II and eHDA *quantitatively* to facilitate critical comparisons with the viscosity of structural glass formers and the plasticity of orientational glasses.

Above all, just below the crystallization line T_X, shown in Fig. 3, dynamical processes in potentially deeply supercooled liquids need to be explored more often by means of *in situ* experiments. For instance, near 150 K and 0.2 GPa amorphous ices should be probed by *in situ* inelastic scattering, *in situ* magnetic resonance, and *in situ* vibrational spectroscopy. So far, most experiments [but not all, see, e.g., Klotz, Strässle, Nelmes *et al.* (2005)] study quench-recovered samples *ex situ* at ambient pressure. The development and application of *in situ* techniques will be instrumental in eventually providing satisfactory answers to long-standing questions regarding the nature of water's molecular mobility above the glass transition temperatures summarized in Fig. 3. Hence, we expect substantial progress regarding the resolution of the water conundrum when refined experimental work along these lines becomes available for appropriately prepared and fully relaxed samples, where necessary.

Likewise, it was argued that the deuteron or proton transfers exploited by Fisher and Devlin (1995) and Smith and Kay (1999) could proceed with similar rates on crystalline as well as on noncrystalline networks. Hence, experiments based on hydrogen isotope exchange may not provide compelling evidence to everyone. We are convinced, though, that diffusion measurements probing the transport of *oxygen* will do the job. One might exploit the minute differences in the neutron scattering lengths of different oxygen isotopes (Fischer *et al.*, 2012) and with an interest in unraveling the oddities of water's bulk glass transitions such highly challenging experiments ought to demonstrate convincingly that *bulk* properties are probed.

Finally, we briefly summarize our position regarding some of the controversial issues. Whereas the vitrified liquid (HGW) represents the most natural reference for glassy water, the debate centering on the nature of the pressure-amorphized ices HDA and LDA is still not settled. From structural data only, for instance from the close similarity of the radial distribution functions of LDA-I, LDA-II, and ASW to those of HGW (see Fig. 8), it is problematic to distinguish between the scenarios depicted in Fig. 2. However, as documented in this Colloquium, there is more and more experimental evidence suggesting that the well-annealed low-density amorphous ices are highly similar to each other not only in terms of structure, but also in terms of their slow, fast, and ultrafast dynamics,

including the solid-liquid glass transition. HDA, by contrast, is very different from the low-density amorphous ices, in terms of structure and in terms of dynamics. The observation that HDA's glass transition is distinct from that of LDA fuels two-liquid scenarios of water. In spite of the controversies and open questions summarized previously we feel that overwhelming experimental evidence supports the idea that distinct, deeply supercooled liquids exist with eHDA and LDA-II (rather than uHDA and LDA-I) as the proxies of the suggested high-density and low-density liquids, respectively. Furthermore, Mishima and Suzuki (2002), Klotz, Strässle, Nelmes *et al.* (2005), and Winkel, Mayer, and Loerting (2011) saw evidence for a first-order nature of the transition. The latter work observes this first-order transition at 140 K, i.e., in the ultraviscous liquid domain above the glass transition temperature, a finding that is suggestive of a first-order liquid-liquid transition similar to the one proposed by Poole *et al.* (1992). These experiments call for additional work, especially using further *in situ* monitoring of the transition. Mainly due to restrictions imposed by the "catastrophic" crystallization occurring when cooling bulk water much below 230 K, by means of laboratory experiments no one seems currently capable of addressing the question directly whether the proposed second critical point scenario is of relevance for understanding the bulk liquid's properties. In order to resolve this question ultrafast heating at rates large enough to avoid ice nucleation and growth in conjunction with simultaneous ultrafast probing under high pressure will be required. Experiments of this type are highly challenging and have not been accomplished so far.

Regarding the interpretation of the theoretical and experimental work that the future holds in stock for us, it is not difficult to predict that controversies will remain, yet, like before, they certainly will create exciting scientific and intellectual adventures, thus opening new avenues in our efforts to grasp ever deeper the beauty and complexity of water. So, despite many recent discoveries and much progress in the field made already, for the time being much remains true of Franks' (1972) judgment that "of all known liquids, water is probably the most studied and least understood."

ACKNOWLEDGMENTS

It is our pleasure to thank Michael Elsaesser, Violeta Fuentes-Landete, Stephan Fuhrmann, Philip H. Handle, Ingrid Kohl, Karsten W. Köster, Sonja Lemke, Florian Löw, Christian Mitterdorfer, Helge Nelson, Marco Scheuermann, Werner Schustereder, Markus Seidl, and Josef Stern who were or are involved in studies of noncrystalline ices in our groups. We also thank numerous collaborators including Livia Bove (UPMC Paris), Daniel Bowron (ISIS), John Finney (UC London), Nicolas Giovambattista (CU New York), Marek Koza (ILL Grenoble), Ranko Richert (Arizona State U), Alexei Sokolov (U Tennessee, Knoxville), and Gerhard Zifferer (U Vienna). Our work relating to this project was financially supported by the Deutsche Forschungsgemeinschaft under Grant No. BO1301, the Austrian Science Fund FWF (Schrödinger-fellowship and Schrödinger-Rückkehrprogramm to T. L., START award No. Y391, Hertha-Firnberg Programm No. T463 to K. A.-W. and bilateral project No. I1392 with ANR France), the European Research Council (ERC Starting Grant SULIWA), and the Alexander von Humboldt Stiftung (Friedrich Wilhelm Bessel award to T. L.).

REFERENCES

Amann-Winkel, K., C. Gainaru, P. H. Handle, M. Seidl, H. Nelson, R. Böhmer, and T. Loerting, 2013, "Water's second glass transition," Proc. Natl. Acad. Sci. U.S.A. **110**, 17720–17725.

Andersson, O., 2005, "Relaxation Time of Water's High-Density Amorphous Ice Phase," Phys. Rev. Lett. **95**, 205503.

Andersson, O., 2008, "Dielectric relaxation of the amorphous ices," J. Phys. Condens. Matter **20**, 244115.

Andersson, O., 2011, "Glass-liquid transition of water at high pressure," Proc. Natl. Acad. Sci. U.S.A. **108**, 11013–11016.

Andersson, O., and A. Inaba, 2006, "Dielectric properties of high-density amorphous ice under pressure," Phys. Rev. B **74**, 184201.

Angell, C. A., 1982, "Supercooled Water," in *Water—a comprehensive treatise*, edited by F. Franks, Water and Aqueous Solutions at Subzero Temperatures Vol. 7 (Plenum, New York), pp. 1–81.

Angell, C. A., 2007, "Glass transition dynamics in water and other tetrahedral liquids: 'order-disorder' transitions versus 'normal' glass transitions," J. Phys. Condens. Matter **19**, 205112.

Angell, C. A., 2008, "Insights into Phases of Liquid Water from Study of Its Unusual Glass-Forming Properties," Science **319**, 582–587.

Angell, C. A., 2014, "Supercooled water: Two phases?," Nat. Mater. **13**, 673–675.

Angell, C. A., C. T. Moynihan, and M. Hemmati, 2000, "'Strong' and 'superstrong' liquids, and an approach to the perfect glass state via phase transition," J. Non-Cryst. Solids **274**, 319–331.

Baragiola, R. A., 2003, "Microporous amorphous water ice thin films: Properties and their astronomical implications," in *Water in Confining Geometries*, edited by V. Buch and J. P. Devlin (Springer-Verlag, Berlin, Heidelberg), pp. 359–395.

Bartell, L., and J. Huang, 1994, "Supercooling of Water below the Anomalous Range near 226 K," J. Phys. Chem. **98**, 7455–7437.

Bellissent-Funel, M. C., L. Bosio, A. Hallbrucker, E. Mayer, and R. Sridi-Dorbez, 1992, "X-ray and neutron scattering studies of the structure of hyperquenched glassy water," J. Chem. Phys. **97**, 1282–1286.

Belosludov, R. V., O. S. Subbotin, H. Mizuseki, P. M. Rodger, Y. Kawazoe, and V. R. Belosludov, 2008, "Crystal-like low frequency phonons in the low-density amorphous and high-density amorphous ices," J. Chem. Phys. **129**, 114507.

Bhabhe, A., H. Pathak, and B. E. Wyslouzil, 2013, "Freezing of heavy water (D_2O) nanodroplets," J. Phys. Chem. A **117**, 5472–5482.

Bhat, M. H., V. Molinero, E. Soignard, V. C. Solomon, S. Sastry, J. L. Yarger, and C. A. Angell, 2007, "Vitrification of a monatomic metallic liquid," Nature (London) **448**, 787–790.

Biddle, J. W., V. Holten, and M. A. Anisimov, 2014, "Behavior of supercooled aqueous solutions stemming from hidden liquid–liquid transition in water," J. Chem. Phys. **141**, 074504.

Binder, K., and A. P. Young, 1986, "Spin-Glasses—Experimental Facts, Theoretical Concepts, and Open Questions," Rev. Mod. Phys. **58**, 801–976.

Bizid, A., L. Bosio, A. Defrain, and M. Oumezzine, 1987, "Structure of high-density amorphous water. I. X-ray diffraction study," J. Chem. Phys. **87**, 2225–2230.

Böhmer, R., K. L. Ngai, C. A. Angell, and D. J. Plazek, 1993, "Nonexponential relaxations in strong and fragile glass formers," J. Chem. Phys. **99**, 4201–4209.

Bowron, D. T., J. L. Finney, A. Hallbrucker, I. Kohl, T. Loerting, E. Mayer, and A. K. Soper, 2006, "The local and intermediate range structures of the five amorphous ices at 80 K and ambient pressure: A Faber-Ziman and Bhatia-Thornton analysis," J. Chem. Phys. **125**, 194502.

Brovchenko, I., A. Geiger, and A. Oleinikova, 2003, "Multiple liquid-liquid transitions in supercooled water," J. Chem. Phys. **118**, 9473-9476.

Brovchenko, I., A. Geiger, and A. Oleinikova, 2005, "Liquid-liquid phase transitions in supercooled water studied by computer simulations of various water models," J. Chem. Phys. **123**, 044515.

Brovchenko, I., and A. Oleinikova, 2008, "Multiple phases of liquid water," Chem. Phys. Chem. **9**, 2660–2675.

Brüggeller, P., and E. Mayer, 1980, "Complete vitrification in pure liquid water and dilute aqueous solutions," Nature (London) **288**, 569–571.

Burke, D. J., and W. A. Brown, 2010, "Ice in space: surface science investigations of the thermal desorption of model interstellar ices on dust grain analogue surfaces," Phys. Chem. Chem. Phys. **12**, 5947–5969.

Burton, E. F., and W. F. Oliver, 1935, "X-ray diffraction patterns of ice," Nature (London) **135**, 505–506.

Capaccioli, S., and K. L. Ngai, 2011, "Resolving the controversy on the glass transition temperature of water?," J. Chem. Phys. **135**, 104504.

Cartwright, J. H. E., B. Escribano, and C. I. Sainz-Diaz, 2008, "The Mesoscale Morphologies of Ice Films: Porous and Biomorphic Forms of Ice under Astrophysical Conditions," Astrophys. J. **687**, 1406–1414.

Caupin, F., 2015, "Escaping the no man's land: Recent experiments on metastable liquid water," J. Non-Cryst. Solids **407**, 441–448.

Chandler, D., 2014, Illusions of phase coexistence: Comments on "Metastable liquid–liquid transition in a molecular model of water," Nature (London) **510**, 385.

Collings, M. P., J. W. Dever, M. R. S. McCoustra, and H. J. Fraser, 2005, *Implications of ice morphology for comet formation, in: Highlights of astronomy* (Astronomical Society Pacific, San Francisco), pp. 491–494.

Debenedetti, P. G., 2003, "Supercooled and glassy water," J. Phys. Condens. Matter **15**, R1669–R1726.

Dowell, L. G., and A. P. Rinfret, 1960, "Low temperature forms of ice as studied by X-ray diffraction," Nature (London) **188**, 1144–1148.

Elsaesser, M. S., K. Winkel, E. Mayer, and T. Loerting, 2010, "Reversibility and isotope effect of the calorimetric glass liquid transition of low-density amorphous ice," Phys. Chem. Chem. Phys. **12**, 708–712.

Fahrenheit, D. G., 1724, "Experimenta & Observationes de Congelatione Aquae in Vacuo Factae," Phil. Trans. R. Soc. London **33**, 78–84.

Finney, J. L., D. T. Bowron, A. K. Soper, T. Loerting, E. Mayer, and A. Hallbrucker, 2002, "Structure of a New Dense Amorphous Ice," Phys. Rev. Lett. **89**, 205503.

Finney, J. L., A. Hallbrucker, I. Kohl, A. K. Soper, and D. T. Bowron, 2002, "Structures of High and Low Density Amorphous Ice by Neutron Diffraction," Phys. Rev. Lett. **88**, 225503.

Fischer, H. E., J. M. Simonson, J. C. Neuefeind, H. Lemmel, H. Rauch, A. Zeidler, and P. S. Salmon, 2012, "The bound coherent neutron scattering lengths of the oxygen isotopes," J. Phys. Condens. Matter **24**, 505105.

Fisher, M., and J. P. Devlin, 1995, "Defect Activity in Amorphous Ice From Isotopic Exchange Data: Insight into the Glass Transition," J. Phys. Chem. **99**, 11584–11590.

Floriano, M. A., Y. P. Handa, D. D. Klug, and E. Whalley, 1989, "Nature of the transformations of ice I and low-density amorphous ice to high-density amorphous ice," J. Chem. Phys. **91**, 7187–7192.

Floriano, M. A., E. Whalley, E. C. Svensson, and V. F. Sears, 1986, "Structure of high-density amorphous ice by neutron diffraction," Phys. Rev. Lett. **57**, 3062–3064.

Franks, F., 1972, "Introduction—Water, The Unique Chemical," in *Water—A comprehensive treatise*, edited by F. Franks, The Physics and Physical Chemistry of Water, Vol. 1 (Plenum, New York), pp. 1–20.

Fuentes-Landete, V., *et al.*, 2015, "Crystalline and amorphous ices," *Water: Fundamentals as the Basis for Understanding the Environment and Promoting Technology* Vol. 187, edited by P. G. Debenedetti, M. A. Ricci, and F. Bruni, in Proceedings of the International School of Physics "Enrico Fermi" (IOS, Amsterdam), pp. 173–208, doi:10.3254/978-1-61499-507-4-173.

Gainaru, C., *et al.*, 2014, "Anomalous Isotope Effect in the Low-Temperature Dynamics of Water," Proc. Natl. Acad. Sci. U.S.A. **111**, 17402–17407.

Geil, B., T. M. Kirschgen, and F. Fujara, 2005, "Mechanism of proton transport in hexagonal ice," Phys. Rev. B **72**, 014304.

Giovambattista, N., C. A. Angell, F. Sciortino, and H. E. Stanley, 2004, "Glass-Transition Temperature of Water: A Simulation Study," Phys. Rev. Lett. **93**, 047801.

Giovambattista, N., T. Loerting, B. R. Lukanov, and F. W. Starr, 2012, "Interplay of the glass transition and the liquid-liquid phase transition in water," Sci. Rep. **2**, 390.

Götz, M., T. Bauer, P. Lunkenheimer, and A. Loidl, 2014, "Supercooled-liquid and plastic-crystalline state in succinonitrile-glutaronitrile mixtures," J. Chem. Phys. **140**, 094504.

Hallbrucker, A., E. Mayer, and G. P. Johari, 1989a, "Glass-liquid transition and the enthalpy of devitrification of annealed vapor-deposited amorphous solid water: a comparison with hyperquenched glassy water," J. Phys. Chem. **93**, 4986–4990.

Hallbrucker, A., E. Mayer, and G. P. Johari, 1989b, "The heat capacity and glass transition of hyperquenched glassy water," Philos. Mag. B **60**, 179–187.

Hallbrucker, A., E. Mayer, L. P. O'Mard, J. C. Dore, and P. Chieux, 1991, "Structural characterization of hyperquenched glassy water and vapor-deposited amorphous ice," Phys. Lett. A **159**, 406–410.

Handa, Y. P., O. Mishima, and E. Whalley, 1986, "High-density amorphous ice. III. Thermal properties," J. Chem. Phys. **84**, 2766–2770.

Handle, P. H., and T. Loerting, 2016, "Dynamics anomaly in high-density amorphous ice between 0.7 and 1.1 GPa," Phys. Rev. B **93**, 064204.

Handle, P. H., M. Seidl, and T. Loerting, 2012, "Relaxation time of high density amorphous ice at 0.1 and 0.2 GPa," Phys. Rev. Lett. **108**, 225901.

Hansen, T. C., A. Falenty, and W. F. Kuhs, 2007, "Modelling ice I_c of different origin and stacking-faulted hexagonal ice using neutron powder diffraction data," in *Physics and Chemistry of Ice*, edited by W. F. Kuhs (RSC Publishing, Cambridge), pp. 201–208.

Hemley, R. J., L. C. Chen, and H. K. Mao, 1989, "New transformations between crystalline and amorphous ice," Nature (London) **338**, 638–640.

Höchli, U. T., K. Knorr, and A. Loidl, 1990, "Orientational Glasses," Adv. Phys. **39**, 405–615.

Holten, V., J. C. Palmer, P. H. Poole, P. G. Debenedetti, and M. A. Anisimov, 2014, "Two-state thermodynamics of the ST2 model for supercooled water," J. Chem. Phys. **140**, 104502.

Ickes, L., A. Welti, C. Hoose, and U. Lohmann, 2015, "Classical nucleation theory of homogeneous freezing of water: thermodynamic and kinetic parameters," Phys. Chem. Chem. Phys. **17**, 5514–5537.

Jenniskens, P., and D. F. Blake, 1994, "Structural transitions in amorphous water ice and astrophysical implications," Science **265**, 753–756.

Jenniskens, P., and D. F. Blake, 1996, "Crystallization of amorphous water ice in the Solar System," Astrophys. J. **473**, 1104–1113.

Johari, G. P., 1998, "Liquid State of Low-Density Pressure-Amorphized Ice above Its T_g," J. Phys. Chem. B **102**, 4711–4714.

Johari, G. P., 2005, "Dielectric relaxation time of bulk water at 136–140 K, background loss and crystallization effects," J. Chem. Phys. **122**, 144508.

Johari, G. P., and O. Andersson, 2007, "Vibrational and relaxational properties of crystalline and amorphous ices," Thermochim. Acta **461**, 14–43.

Johari, G. P., G. Fleissner, A. Hallbrucker, and E. Mayer, 1994, "Thermodynamic continuity between glassy and normal water," J. Phys. Chem. **98**, 4719–4725.

Johari, G. P., and M. Goldstein, 1970, "Viscous liquids and the glass transition. II. Secondary relaxations in glasses of rigid molecules," J. Chem. Phys. **53**, 2372–2388.

Johari, G. P., A. Hallbrucker, and E. Mayer, 1987, "The glass-liquid transition of hyperquenched water," Nature (London) **330**, 552–553.

Johari, G. P., A. Hallbrucker, and E. Mayer, 1991, "Isotope and impurity effects on the glass transition and crystallization of pressure-amorphized hexagonal and cubic ice," J. Chem. Phys. **95**, 6849–6855.

Johari, G. P., and E. Whalley, 1981, "The Dielectric Properties of Ice I_h in the Range 272–133 K," J. Chem. Phys. **75**, 1333–1340.

Johnson, W. L., 1999, "Bulk Glass-Forming Metallic Alloys: Science and Technology," MRS Bull. **24**, 42–56.

Johnson, W. L., G. Kaltenboeck, M. D. Demetriou, J. P. Schramm, X. Liu, K. Samwer, C. P. Kim, and D. C. Hofmann, 2011, "Beating Crystallization in Glass-Forming Metals by Millisecond Heating and Processing," Science **332**, 828–833.

Kauzmann, W., 1948, "The nature of the glassy state and the behavior of liquids at low temperatures," Chem. Rev. **43**, 219–256.

Kiselev, S. B., and J. F. Ely, 2003, "Physical limit of stability in supercooled D_2O and $D_2O + H_2O$ mixtures," J. Chem. Phys. **118**, 680–689.

Klotz, S., G. Hamel, J. S. Loveday, R. J. Nelmes, and M. Guthrie, 2003, "Recrystallisation of HDA ice under pressure by in-situ neutron diffraction to 3.9 GPa," Z. Kristallogr. **218**, 117–122.

Klotz, S., T. Strässle, R. J. Nelmes, J. S. Loveday, G. Hamel, G. Rousse, B. Canny, J. C. Chervin, and A. M. Saitta, 2005, "Nature of the Polyamorphic Transition in Ice under Pressure," Phys. Rev. Lett. **94**, 025506.

Klotz, S., T. Strässle, A. M. Saitta, G. Rousse, G. Hamel, R. J. Nelmes, J. S. Loveday, and M. Guthrie, 2005, "In situ neutron diffraction studies of high density amorphous ice under pressure," J. Phys. Condens. Matter **17**, S967–S974.

Kohl, I., L. Bachmann, A. Hallbrucker, E. Mayer, and T. Loerting, 2005, "Liquid-like relaxation in hyperquenched water at ≤ 140 K," Phys. Chem. Chem. Phys. **7**, 3210–3220.

Kohl, I., L. Bachmann, E. Mayer, A. Hallbrucker, and T. Loerting, 2005, "Glass transition in hyperquenched water?," Nature (London) **435**, E1–E2.

Kolesnikov, A. I., J. C. Li, N. C. Ahmad, C. K. Loong, J. Nipko, D. Yocum, and S. F. Parker, 1999, "Neutron spectroscopy of high-density amorphous ice," Physica B (Amsterdam) **263–264**, 650–652.

Kouchi, A., and T. Kuroda, 1990, "Amorphization of Cubic Ice by Ultraviolet-Irradiation," Nature (London) **344**, 134–135.

Koza, M. M., 2008, "Vibrational dynamics of amorphous ice structures studied by high-resolution neutron spectroscopy," Phys. Rev. B **78**, 064303.

Koza, M. M., 2009, "Transient Pronounced Density Variation in Amorphous Ice Structures," Z. Phys. Chem. **223**, 979–1000.

Koza, M. M., B. Geil, M. Scheuermann, H. Schober, G. Monaco, and H. Requardt, 2008, "Vibrational dynamics of very high density amorphous ice studied by high-resolution x-ray spectroscopy," Phys. Rev. B **78**, 224301.

Koza, M. M., H. Schober, B. Geil, M. Lorenzen, and H. Requardt, 2004, "Crystalline inelastic response of high-density amorphous ice," Phys. Rev. B **69**, 024204.

Kudlik, A., S. Benkhof, T. Blochowicz, C. Tschirwitz, and E. Rössler, 1999, "The dielectric response of simple organic glass formers," J. Mol. Struct. **479**, 201–218.

Kuhs, W. F., C. Sippel, A. Falenty, and T. C. Hansen, 2012, "Extent and Relevance of Stacking Disorder in "Ice I_c"," Proc. Natl. Acad. Sci. U.S.A. **109**, 21259–21264.

Laksmono, H., *et al.*, 2015, "Anomalous behavior of the homogeneous ice nucleation rate in "no-man's land"," J. Phys. Chem. Lett. **6**, 2826–2832.

Lemke, S., *et al.*, 2014 (unpublished).

Li, J. C., and P. Jenniskens, 1997, "Inelastic neutron scattering study of high-density amorphous water ice," Planet. Space Sci. **45**, 469–473.

Limmer, D. T., and D. Chandler, 2011, "The putative liquid–liquid transition is a liquid-solid transition in atomistic models of water," J. Chem. Phys. **135**, 134503.

Limmer, D. T., and D. Chandler, 2013, "The putative liquid–liquid transition is a liquid–solid transition in atomistic models of water. II," J. Chem. Phys. **138**, 214504.

Limmer, D. T., and D. Chandler, 2014, "Theory of amorphous ices," Proc. Natl. Acad. Sci. U.S.A. **111**, 9413–9418.

Loerting, T., V. Fuentes-Landete, P. H. Handle, M. Seidl, K. Amann-Winkel, C. Gainaru, and R. Böhmer, 2015, "The glass transition in high-density amorphous ice," J. Non-Cryst. Solids **407**, 423–430.

Loerting, T., I. Kohl, C. Salzmann, E. Mayer, and A. Hallbrucker, 2002, "(Meta-)stability domain of ice XII revealed between $\approx$158–212 K and $\approx$0.7–1.5 GPa on isobaric heating of high-density amorphous ice," J. Chem. Phys. **116**, 3171–3174.

Loerting, T., C. Salzmann, I. Kohl, E. Mayer, and A. Hallbrucker, 2001, "A second distinct structural state of high-density amorphous ice at 77 K and 1 bar," Phys. Chem. Chem. Phys. **3**, 5355–5357.

Loerting, T., K. Winkel, M. Seidl, M. Bauer, C. Mitterdorfer, P. H. Handle, C. G. Salzmann, E. Mayer, J. L. Finney, and D. T. Bowron, 2011, "How many amorphous ices are there?," Phys. Chem. Chem. Phys. **13**, 8783–8794.

Löw, F., K. Amann-Winkel, B. Geil, T. Loerting, C. Wittich, and F. Fujara, 2013, "Limits of metastability in amorphous ices: ^{2}H-NMR relaxation," Phys. Chem. Chem. Phys. **15**, 576–580.

Löw, F., K. Amann-Winkel, T. Loerting, F. Fujara, and B. Geil, 2013, "Ultra-slow Dynamics in Low Density Amorphous Ice Revealed by Deuteron NMR: Indications for a Glass Transition," Phys. Chem. Chem. Phys. **15**, 9308–9314.

Malkin, T. L., B. J. Murray, C. Salzmann, V. Molinero, S. J. Pickering, and T. Whale, 2015, "Stacking disorder in ice I," Phys. Chem. Chem. Phys. **17**, 60–76.

Mallamace, F., C. Corsaro, S.-H. Chen, and H. E. Stanley, 2013, "Transport and dynamics in supercooled confined water," Adv. Chem. Phys. **152**, 203–262.

Manka, A., H. Pathak, S. Tanimura, J. Wölk, R. Strey, and B. E. Wyslouzil, 2012, "Freezing water in no-man's land," Phys. Chem. Chem. Phys. **14**, 4505–4516.

Mayer, E., 1985, "New method for vitrifying water and other liquids by rapid cooling of their aerosols," J. Appl. Phys. **58**, 663–667.

Mayer, E., and P. Brüggeller, 1982, "Vitrification of pure liquid water by high-pressure jet freezing," Nature (London) **298**, 715–718.

Mayer, E., and R. Pletzer, 1987, "Amorphous ice, a microporous solid: Astrophysical implications," J. Phys. Colloq. **48**, C1-581–C1-586.

McClure, S. M., D. J. Safarik, T. M. Truskett, and C. B. Mullins, 2006, "Evidence that Amorphous Water below 160 K Is Not a Fragile Liquid," J. Phys. Chem. B **110**, 11033–11036.

McMillan, J. A., and S. C. Los, 1965, "Vitreous ice: Irreversible transformations during warm-up," Nature (London) **206**, 806–807.

McMillan, P. F., M. Wilson, M. C. Wilding, D. Daisenberger, M. Mezouar, and G. N. Greaves, 2007, "Polyamorphism and liquid–liquid phase transitions: challenges for experiment and theory," J. Phys. Condens. Matter **19**, 415101.

Mishima, O., 1994, "Reversible first-order transition between two H_2O amorphs at ∼0.2 GPa and ∼135 K," J. Chem. Phys. **100**, 5910–5912.

Mishima, O., 2004, "The glass-to-liquid transition of the emulsified high-density amorphous ice made by pressure-induced amorphization," J. Chem. Phys. **121**, 3161–3164.

Mishima, O., L. D. Calvert, and E. Whalley, 1984, "Melting ice I at 77 K and 10 kbar: a new method of making amorphous solids," Nature (London) **310**, 393–395.

Mishima, O., L. D. Calvert, and E. Whalley, 1985, "An apparently first-order transition between two amorphous phases of ice induced by pressure," Nature (London) **314**, 76–78.

Mishima, O., and H. E. Stanley, 1998a, "Decompression-induced melting of ice IV and the liquid-liquid transition in water," Nature (London) **392**, 164–168.

Mishima, O., and H. E. Stanley, 1998b, "The relationship between liquid, supercooled and glassy water," Nature (London) **396**, 329–335.

Mishima, O., and Y. Suzuki, 2001, "Vitrification of emulsified liquid water under pressure," J. Chem. Phys. **115**, 4199–4202.

Mishima, O., and Y. Suzuki, 2002, "Propagation of the polyamorphic transition of ice and the liquid–liquid critical point," Nature (London) **419**, 599–603.

Mitterdorfer, C., M. Bauer, T. G. A. Youngs, D. T. Bowron, C. R. Hill, H. J. Fraser, J. L. Finney, and T. Loerting, 2014, "Small-angle neutron scattering study of micropore collapse in amorphous solid water," Phys. Chem. Chem. Phys. **16**, 16013–16020.

Monaco, G., C. Masciovecchio, G. Ruocco, and F. Sette, 1998, "Determination of the infinite frequency sound velocity in the glass former o-terphenyl," Phys. Rev. Lett. **80**, 2161–2164.

Moon, E., Y. Kim, S. Shin, and H. Kang, 2012, "Asymmetric Transport Efficiencies of Positive and Negative Ion Defects in Amorphous Ice," Phys. Rev. Lett. **108**, 226103.

Moore, E. B., and V. Molinero, 2011, "Structural transformation in supercooled water controls the crystallization rate of ice," Nature (London) **479**, 506–508.

Murray, B. J., D. O'Sullivan, J. D. Atkinson, and M. E. Webb, 2012, "Ice nucleation by particles immersed in supercooled cloud droplets," Chem. Soc. Rev. **41**, 6519–6554.

Narten, A. H., and H. A. Levy, 1971, "Liquid water – molecular correlation functions from x-ray diffraction," J. Chem. Phys. **55**, 2263-2269.

Nelmes, R. J., J. S. Loveday, T. Straessle, C. L. Bull, M. Guthrie, G. Hamel, and S. Klotz, 2006, "Annealed high-density amorphous ice under pressure," Nat. Phys. **2**, 414–418.

Nielsen, A. I., T. Christensen, B. Jakobsen, K. Niss, N. B. Olsen, R. Richert, and J. C. Dyre, 2009, "Prevalence of approximate $\sqrt{t}$ relaxation for the dielectric α process in viscous organic liquids," J. Chem. Phys. **130**, 154508.

Novikov, V. N., and A. P. Sokolov, 2013, "Role of quantum effects in the glass transition," Phys. Rev. Lett. **110**, 065701.

Pallares, G., M. El Mekki Azouzi, M. A. González, J. L. Aragones, J. L. F. Abascal, C. Valeriani, and F. Caupin, 2014, "Anomalies in bulk supercooled water at negative pressure," Proc. Natl. Acad. Sci. U.S.A. **111**, 7936–7941.

Palmer, J. C., P. G. Debenedetti, R. Car, and A. Z. Panagiotopoulos, 2014, "Response to Comment [arXiv:1407.6854] on Palmer *et al.*," Nature (London) **510**, 385.

Palmer, J. C., F. Martelli, Y. Liu, R. Car, A. Z. Panagiotopoulos, and P. G. Debenedetti, 2014, "Metastable liquid–liquid transition in a molecular model of water," Nature (London) **510**, 385–388.

Parmentier, A., J. J. Shephard, G. Romanelli, R. Senesi, C. G. Salzmann, and C. Andreani, 2015, "Evolution of Hydrogen Dynamics in Amorphous Ice with Density," J. Phys. Chem. Lett. **6**, 2038–2042.

Paschek, D., A. Rüppert, and A. Geiger, 2008, "Thermodynamic and Structural Characterization of the Transformation from a Metastable Low-Density to a Very High-Density Form of Supercooled TIP4P-Ew Model Water," ChemPhysChem **9**, 2737–2741.

Petrenko, V. F., and R. W. Whitworth, 1999, *Physics Of Ice* (University Press, Oxford).

Phillips, J. C., 1982, "The Physics of Glass," Phys. Today **35**, No. 2, 27–33.

Ponyatovsky, E. G., and V. V. Sinitsyn, 1999, "Thermodynamics of stable and metastable equilibria in water in the T-P region," Physica (Amsterdam) **265B**, 121–127.

Poole, P. H., R. K. Bowles, I. Saika-Voivod, and F. Sciortino, 2013, "Free energy surface of ST2 water near the liquid-liquid phase transition," J. Chem. Phys. **138**, 034505.

Poole, P. H., F. Sciortino, U. Essmann, and H. E. Stanley, 1992, "Phase behaviour of metastable water," Nature (London) **360**, 324–328.

Rasmussen, D. H., and A. P. MacKenzie, 1971, "Glass transition in amorphous water. Application of the measurements to problems arising in cryobiology," J. Phys. Chem. **75**, 967–973.

Rebelo, L. P. N., P. G. Debenedetti, and S. Sastry, 1998, "Singularity-free interpretation of the thermodynamics of supercooled water. II. Thermal and volumetric behavior," J. Chem. Phys. **109**, 626–633.

Ripmeester, J. A., C. I. Ratcliffe, and D. D. Klug, 1992, "A ^{1}H and ^{2}H nuclear magnetic resonance study of amorphous ices at 77 K," J. Chem. Phys. **96**, 8503–8506.

Roland, C. M., S. Hensel-Bielowka, M. Paluch, and R. Casalini, 2005, "Supercooled dynamics of glass-forming liquids and polymers under hydrostatic pressure," Rep. Prog. Phys. **68**, 1405–1478.

Ruocco, G., and F. Sette, 2001, "High-frequency vibrational dynamics in glasses," J. Phys. Condens. Matter **13**, 9141–9164.

Russo, J., F. Romano, and H. Tanaka, 2014, "New metastable form of ice and its role in the homogeneous crystallization of water," Nat. Mater. **13**, 733–739.

Salzmann, C. G., I. Kohl, T. Loerting, E. Mayer, and A. Hallbrucker, 2003a, "The low-temperature dynamics of recovered ice XII as studied by differential scanning calorimetry: a comparison with ice V," Phys. Chem. Chem. Phys. **5**, 3507–3517.

Salzmann, C. G., I. Kohl, T. Loerting, E. Mayer, and A. Hallbrucker, 2003b, "Pure ices IV and XII from high-density amorphous ice," Can. J. Phys. **81**, 25–32.

Salzmann, C. G., P. G. Radaelli, B. Slater, and J. L. Finney, 2011, "The polymorphism of ice: five unresolved questions," Phys. Chem. Chem. Phys. **13**, 18468–18480.

Sartori, N., J. Bednar, and J. Dubochet, 1996, "Electron-beam-induced amorphization of ice III or IX obtained by high-pressure freezing," J. Microsc. **182**, 163–168.

Sastry, S., P. G. Debenedetti, F. Sciortino, and H. E. Stanley, 1996, "Singularity-free interpretation of the thermodynamics of supercooled water," Phys. Rev. E **53**, 6144–6154.

Scheuermann, M., B. Geil, K. Winkel, and F. Fujara, 2006, "Deuteron spin lattice relaxation in amorphous ices," J. Chem. Phys. **124**, 224503.

Schober, H., M. M. Koza, A. Tölle, C. Masciovecchio, F. Sette, and F. Fujara, 2000, "Crystal-like high-frequency phonons in the amorphous phases of solid water," Phys. Rev. Lett. **85**, 4100–4103.

Seidl, M., K. Amann-Winkel, P. H. Handle, G. Zifferer, and T. Loerting, 2013, "From parallel to single crystallization kinetics in high-density amorphous ice," Phys. Rev. B **88**, 174105.

Seidl, M., M. S. Elsaesser, K. Winkel, G. Zifferer, E. Mayer, and T. Loerting, 2011, "Volumetric study consistent with a glass-to-liquid transition in amorphous ices under pressure," Phys. Rev. B **83**, 100201.

Seidl, M., A. Fayter, J. N. Stern, G. Zifferer, and T. Loerting, 2015, "Shrinking water's "no man's land" by lifting its low-temperature boundary," Phys. Rev. B **91**, 144201.

Sellberg, J. A., *et al.*, 2014, "Ultrafast X-ray probing of water structure below the homogeneous ice nucleation temperature," Nature (London) **510**, 381–384.

Sepúlveda, A., E. Leon-Gutierrez, M. Gonzalez-Silveira, C. Rodriguez-Tinoco, M. T. Clavaguera-Mora, and J. Rodriguez-Viejo, 2012, "Glass transition in ultrathin films of amorphous solid water," J. Chem. Phys. **137**, 244506.

Shalit, A., A. F. Perakis, and P. Hamm, 2013, "Two-Dimensional Infrared Spectroscopy of Isotope-Diluted Low Density Amorphous Ice," J. Phys. Chem. B **117**, 15512–15518.

Shephard, J. J., J. S. O. Evans, and C. G. Salzmann, 2013, "Structural Relaxation of Low-Density Amorphous Ice upon Thermal Annealing," J. Phys. Chem. Lett. **4**, 3672–3676.

Shpakov, V. P., P. M. Rodger, J. S. Tse, D. D. Klug, and V. R. Belosludov, 2002, "Thermodynamic Discontinuity between Low-Density Amorphous Ice and Supercooled Water," Phys. Rev. Lett. **88**, 155502.

Simeoni, G. G., T. Bryk, F. A. Gorelli, M. Krisch, G. Ruocco, M. Santoro, and T. Scopigno, 2010, "The Widom line as the crossover between liquid-like and gas-like behaviour in supercritical fluids," Nat. Phys. **6**, 503–507.

Smith, R. S., Z. Dohnalek, G. A. Kimmel, G. Teeter, P. Ayotte, J. L. Daschbach, and B. D. Kay, 2003, "Molecular beam studies of nanoscale films of amorphous solid water," in *Water in Confining Geometries*, edited by V. Buch and J. P. Devlin (Springer-Verlag, Berlin, Heidelberg), pp. 337–357.

Smith, R. S., and B. D. Kay, 1999, "The existence of supercooled liquid water at 150 K," Nature (London) **398**, 788–791.

Soper, A. K., 2008, "Structural transformations in amorphous ice and supercooled water and their relevance to the phase diagram of water," Mol. Phys. **106**, 2053–2076.

Soper, A. K., 2014, "Supercooled water: Continuous trends," Nat. Mater. **13**, 671–673.

Speedy, R. J., 1982, "Stability-limit conjecture. An interpretation of the properties of water," J. Phys. Chem. **86**, 982–991.

Speedy, R. J., and C. A. Angell, 1976, "Isothermal compressibility of supercooled water and evidence for a thermodynamic singularity at −45 °C," J. Chem. Phys. **65**, 851–858.

Stanley, H. E., S. V. Buldyrev, M. Canpolat, O. Mishima, M. R. Sadr-Lahijany, A. Scala, and F. W. Starr, 2000, "The puzzling behavior of water at very low temperature," Phys. Chem. Chem. Phys. **2**, 1551–1558.

Stevenson, K. P., G. A. Kimmel, Z. Dohnalek, R. S. Smith, and B. D. Kay, 1999, "Controlling the morphology of amorphous solid water," Science **283**, 1505–1507.

Strazzulla, G., G. A. Baratta, G. Leto, and G. Foti, 1992, "Ion-beam-induced amorphization of crystalline water ice," Europhys. Lett. **18**, 517–522.

Tainter, C. J., L. Shi, and J. L. Skinner, 2014, "Structure and OH-stretch spectroscopy of low- and high-density amorphous ices," J. Chem. Phys. **140**, 134503.

Tanaka, H., 1996, "Phase behaviors of supercooled waters: Reconciling a critical point of amorphous ices with spinodal instability," J. Chem. Phys. **105**, 5099–5111.

Tulk, C. A., C. J. Benmore, J. Urquidi, D. D. Klug, J. Neuefeind, B. Tomberli, and P. A. Egelstaff, 2002, "Structural Studies of Several Distinct Metastable Forms of Amorphous Ice," Science **297**, 1320–1323.

Urquidi, J., C. J. Benmore, P. A. Egelstaff, M. Guthrie, S. E. McLain, C. A. Tulk, D. D. Klug, and J. F. C. Turner, 2004, "A structural comparison of supercooled water and intermediate density amorphous ices," Mol. Phys. **102**, 2007–2014.

Venkatesh, C. G., S. A. Rice, and A. H. Narten, 1974, "Amorphous solid water. X-ray diffraction study," Science **186**, 927–928.

Whalley, E., 1984, "Energies of the phases of ice at zero temperature and pressure," J. Chem. Phys. **81**, 4087–4092.

Whalley, E., D. D. Klug, M. A. Floriano, E. C. Svensson, and V. F. Sears, 1987, "Recent work on high-density amorphous ice," J. Phys. Colloq. **48**, C1-429–C1-434.

Whalley, E., D. D. Klug, and Y. P. Handa, 1989, "Entropy of amorphous ice," Nature (London) **342**, 782–783.

Wilson, G. J., R. K. Chan, D. W. Davidson, and E. Whalley, 1965, "Dielectric Properties of Ices II, III, V, and VI," J. Chem. Phys. **43**, 2384–2391.

Winkel, K., D. T. Bowron, T. Loerting, E. Mayer, and J. L. Finney, 2009, "Relaxation effects in low density amorphous ice: Two distinct structural states observed by neutron diffraction," J. Chem. Phys. **130**, 204502.

Winkel, K., E. Mayer, and T. Loerting, 2011, "Equilibrated High-Density Amorphous Ice and its First-Order Transition to the Low-Density Form," J. Phys. Chem. B **115**, 14141–14148.

Winkel, K., W. Schustereder, I. Kohl, C. G. Salzmann, E. Mayer, and T. Loerting, 2007, "Isothermal Amorphous-Amorphous-Amorphous Transitions in Water," in *Physics and Chemistry of Ice*, edited by W. F. Kuhs (RSC Publishing, Cambridge), pp. 641–648.

Yue, Y. Z., S. L. Jensen, and J. deC. Christiansen, 2002, "Physical aging in a hyperquenched glass," Appl. Phys. Lett. **81**, 2983–2985.

Zarzycki, J., 1991, *Glasses and the vitreous state* (Cambridge University Press, Cambridge, UK).